

Chapter III

THE RAD1 and RAD2 RECEIVERS

DOI	https://doi.org/10.25935/vps6-jb33
Publisher	MASER/PADC
Citation	Sitruk, L. & Manning, R. (2022) <i>The GGS/WIND/Waves Experiment</i> – Chapter 3 (Version 4.3, translated by A. Fave). MASER/PADC. doi:10.25935/VPS6-JB33
License	CC-BY-4.0

Summary

The RAD1 and RAD2 receivers are super-heterodyne radio receivers intended for the analysis of solar and planetary radio bursts. They are in the continuity of the receivers developed in the framework of the ISEE3/SBH and ULYSSE/URAP experiments of DESPA. The frequency range is from 20 to 1040 kHz for RAD1 and from 1.075 to 13.825 MHz for RAD2. The frequency increment step is 4 kHz for RAD1 and 50 kHz for RAD2. The nominal analysis bandwidths are 3 kHz for RAD1 and 20 kHz for RAD2. The RAD1 receiver is connected to the E_x (or possibly E_y) and E_z antennas, the RAD2 receiver to the E_y and E_z antennas. Because of its high frequency range, the RAD2 receiver is intended for the study of the upper solar corona: it bridges the frequency limit of the ground-based instruments and the frequency ranges studied so far. The analysis electronics consist of a VCO-based frequency synthesizer, frequency filters, phase shifters, an automatic gain control circuit, and a voltage-to-frequency analog-to-digital converter. The two RAD1/2 receivers operate essentially in list mode (16 or 32 frequencies selected from 256) or in linear sweep mode (typically 256 frequencies distributed linearly, for type III burst characterization). The list scan mode is implemented by selecting a pointer table and a frequency list. In memory are stored 8 frequency lists corresponding to different criteria (linear or logarithmic scaling, Ulysses lists). To measure both the direction and the polarization of the sources, the synthetic dipole method is used, which combines axial and equatorial antennas. The monitoring of type III bursts, tracers of the magnetic field lines, allows a large-scale mapping of the interplanetary magnetic field.

Content

3. THE RAD1 and RAD2 RECEIVERS	84
3.1. Types of events detected by the RAD1 and RAD2 receivers.....	84
3.2. RAD1 and RAD2 receiver characteristics	85
3.2.1. The RAD1 receiver (RADio receiver band 1).....	85
3.2.2. The RAD2 receiver (RADio receiver band 2).....	85
3.2.3. Equivalent noise bandwidth.....	86
3.2.4. Physical units	87
3.3. The acquisition circuit.....	88
3.3.1. The frequency synthesizer.....	88
3.3.2. Signal transposition.....	89
3.3.3. Selective filtering - Second frequency transposition.....	90
3.3.4. Phase shifters	91
3.3.5. Automatic gain control	92
3.3.6. Analog-to-digital conversion	93
3.4. Direction and polarization of sources: synthetic dipole technique	96
3.4.1. General principle.....	96
3.4.2. The Mathematical Method	97
3.5. Measurement acquisition RAD1/2.....	102
3.5.1. The different modes of acquisition.....	102
3.5.2. Linear sweep mode	104
3.5.3. The list sweep mode	106
3.5.4. List of "items" for RAD1/2 receivers	128

3. THE RAD1 and RAD2 RECEIVERS

3.1. Types of events detected by the RAD1 and RAD2 receivers

The RAD1 and RAD2 instruments are designed to measure the characteristics of radio waves¹ and plasma waves emitted in the regions overflowed by the probe. These waves include (see glossary):

- **Solar bursts**

- Type III solar bursts. These very frequent events appear most often grouped. They are the most observed solar emissions below 1 MHz.
- Type II solar bursts, much less frequent than the previous ones².
- S.A. ("Shock Accelerated" bursts)³.

- **Terrestrial emissions**

- AKR⁴ (Auroral Kilometric Radiation), in the 50 to 600 Hz frequency band.
- Non-Thermal Continuum (NTC) radiation, below about 100 kHz⁵.
- ITKR (Isotropic Terrestrial Kilometric Radiation).
- LF (Low Frequency bursts)⁶.

- **Jovian emissions**

The planet Jupiter emits extremely intense radio waves with, in ascending order of frequency ranges:

- The kilometric emission from Io torus: nKOM ("narrow band kilometric emission"), of narrow frequency band around 100 kHz.
- bKOM ("broad band kilometric emission"), a broadband emission from less than 100 kHz to 400 kHz or more, hectometric HOM (about 40 kHz to a few MHz), and decametric DAM (about 100 kHz to more than 20 MHz).

¹ The frequency range of the RAD1 and RAD2 instruments allows tracking of energetic particle shocks and fluxes from three or four solar radii to one AU.

² These bursts are emitted by electrons accelerated at the level of a shock wave propagating in the solar wind. Due to the speed of the shocks, the frequency drift is much slower than for type III bursts. At RAD1 frequencies, these bursts typically drift from 1 MHz to 10 kHz in about a day, which corresponds to the motion of shock waves in the solar wind. To date, the Waves experiment has detected very few of them (see for example the event of 8/1/97). These events are obviously more frequent during the solar cycle.

³ These bursts are associated with Type IIs emitted near the Sun. One such event was observed on May 6, 1996.

⁴ Still called TKR: Terrestrial Kilometric Radiation.

⁵ The AKR emission and the non-thermal continuous emission are the two main components of the non-thermal terrestrial radio spectrum.

⁶ These bursts have similarities with the ITKR radiation and the quasi-periodic Jovian bursts.

- **Thermal noise**

- The RAD1/2 receivers can be used to supplement the TNR instrument for thermal noise analysis.

3.2. RAD1 and RAD2 receiver characteristics

A schematic diagram of the individual electronic components of the RAD1/2 receivers is given below⁷ (fig).

3.2.1. The RAD1 receiver (RADio receiver band 1)

The RAD1 ("type III" receiver) consists of two super-heterodyne analogue sub-receivers covering the range 20 kHz to 1040 kHz.

One of the sub-receivers is connected to the axial electrical antenna E_z , the other to the "sum" of the antennas E_z and (E_x or E_y). This summation can be disabled. By default the combination is ($E_z, E_x + E_z$), but the combination ($E_z, E_y + E_z$) can also be chosen by remote control, in case of failure of the E_x antenna. The characteristics of the RAD1 receiver are as follows:

Dynamics	approx. 70-80 dB
Bandwidth (nominal value)	3 kHz
Frequency increment	4 kHz
IF frequency	10,684 MHz
Fluctuations	0.2 dB
Frequency of the 2 nd L.O.	10,600 MHz
Equivalent noise bandwidth (S-filter)	3,48 kHz
Equivalent noise bandwidth (Z-filter)	3,37 kHz

3.2.2. The RAD2 receiver (RADio receiver band 2)

This receiver is very similar to the RAD1 receiver, but has a much higher frequency range: 1.075 to 13.825 MHz. This was designed to allow the analysis of the high solar corona ("high corona" receiver).

This receiver acquires the signal from the shorter⁸ of the two antennas E_x and E_y , in this case E_y , as well as the signal from the E_z antenna. The characteristics of the RAD2 receiver are as follows:

Dynamics	approx. 70 dB
Bandwidth ⁹ at 3 dB	20 kHz
Frequency increment	50 kHz
IF frequency	21,425 MHz
Frequency of 2nd L.O.	21,300 MHz
Fluctuations	0,24 dB
Equivalent noise bandwidth (S channel filter)	19 kHz (to be refined)
Equivalent noise bandwidth (channel filter)	19 kHz (to be refined)

⁷ The RAD1/2 receivers (especially RAD2) are similar to those designed for the TSS/RETE mission.

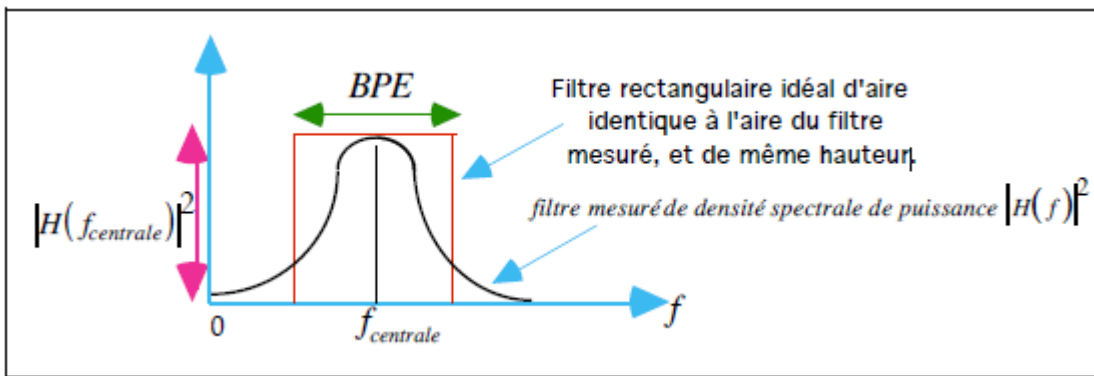
⁸ Remember: the short antenna is suitable for high frequencies.

⁹ The choice of bandwidth for RAD2 takes into account the frequencies of the satellite's converters (more precisely, the frequencies of the spectral interference at harmonic frequencies of 50 Hz. These components are powerful even at high harmonic frequencies: the wider the bandwidth chosen for RAD2, the greater the risk of interference.

3.2.3. Equivalent noise bandwidth

The signals obtained at the output of the receiver are acquired through a bandpass filter. There is therefore a frequency integration. The digital values of these signals must therefore be related¹⁰ to the bandwidth of the filters. This gives values in $Volt^2.Hertz^{-1}$ for power, or $Volt.Hertz^{-1/2}$ for amplitude.

The nominal values of the 3 dB bandwidth of the filters present on each channel (S and Z) are provided by the manufacturer. The shape of these filters is measured using a white noise generator¹¹ (see Chapter 5). By definition, the equivalent noise bandwidth BPE is the width of the rectangle (ideal low-pass filter of rectangular shape) centered on the central frequency f , of the same height as the measured filter of transfer function $H(f)$, and of identical area.



The height of the rectangle being $|H(f_{centrale})|^2$ and its width being BPE , we deduce:

$$BPE = \frac{1}{|H(f_{centrale})|^2} \int_0^{\infty} |H(f)|^2 df$$

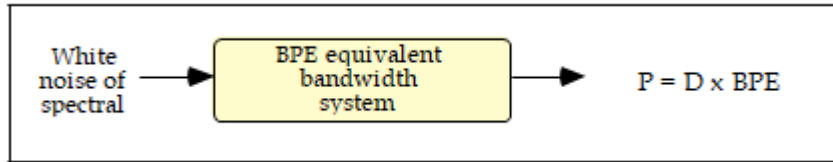
In both cases, the same total output noise power is obtained when the input noise is white. Let D be the power spectral density (PSD) of the input signal, which is white noise. This PSD is expressed in $Volt^2/Hertz$. The output will be the noise power P , expressed in $Volt^2$:

$$P = BPE \cdot D$$

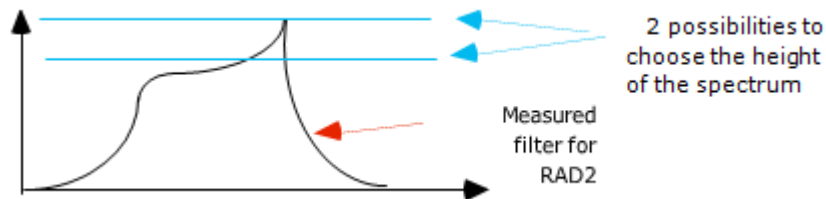
The numerical values of the GHPs are given in the previous section.

¹⁰ This ratio, which does not take into account the distribution of the signal in the band, obviously only makes sense if the bandwidth is small.

¹¹ A noise is said to be white when all frequencies in its spectrum are represented with the same intensity (flat spectrum).



For the RAD2 receiver, the shape of the filter is different from that of the RAD1 receiver, due to a lack of development at the time of design: the shape of the spectrum is such that one can wonder about the height to be taken into account in the calculation of the equivalent noise bandwidth. This problem is currently being addressed.



3.2.4. Physical units

We have seen in the previous § that data can be expressed in $Volt^2 \cdot Hertz^{-1}$ or $Volt \cdot Hertz^{-1/2}$. The software library proposes the following physical units for RAD1/2 instruments:

- dB volts
- $\mu Volt / \sqrt{Hertz}$ at the level of PA.
- SFU : Solar Flux Units
- $\log(SFU)$
- $Watt \cdot m^{-2} \cdot Hz^{-1}$
- $\log(Watt \cdot m^{-2} \cdot Hz^{-1})$

By definition (see appendices): $1 SFU = 10^{-22} Watt \cdot m^{-2} \cdot Hz^{-1}$

The conversion from $Volt^2/Hertz$ to SFU units is obtained using the following formula:

$$Valeur\ en\ SFU = \frac{3 \cdot (valeur\ en\ Volt^2/Hertz)}{C_{eff} \cdot 10^{-22}}$$

From this it follows that the conversion of $\mu Volt / \sqrt{Hertz}$ to SFU units is written:

$$Valeur\ en\ SFU = \frac{3 \cdot (valeur\ en\ \mu Volt / \sqrt{Hertz})^2 \cdot 10^{-12}}{C_{eff} \cdot 10^{-22}}$$

If we note:

$$dB = 10 \log_{10}(\text{valeur en Volt}^2/\text{Hertz})$$

We also have:

$$\text{Valeur en SFU} = \frac{3 \cdot 10^{dB/10}}{C_{eff} \cdot 10^{-22}}$$

C_{eff} is the effective capacity of the antenna, which is written:

$$C_{eff} = \left(\frac{C_a \cdot L}{C_a + C_b} \right)^2 \cdot Z_0$$

C_b : Base capacitance (this is a parasitic capacity).

C_a : Antenna capacitance.

L : Length of the dipole.

Z_0 : impedance of the vacuum which is $120\pi = 377\Omega$.

3.3. The acquisition circuit

3.3.1. The frequency synthesizer

The signal of the S or Z channel, after pre-amplification, is mixed (non-linear device) with a signal provided by a frequency synthesizer.

The frequency synthesizer is a loop circuit based on a variable frequency oscillator (VCO: Voltage Controlled Oscillator). A VCO circuit generates a square wave signal at a given frequency: this frequency depends on the set voltage applied to it. The value of this frequency is changed by changing the value of the voltage applied to the VCO. It is the DPU that indicates the frequency to be synthesized: it is possible here to generate 256 different frequencies.

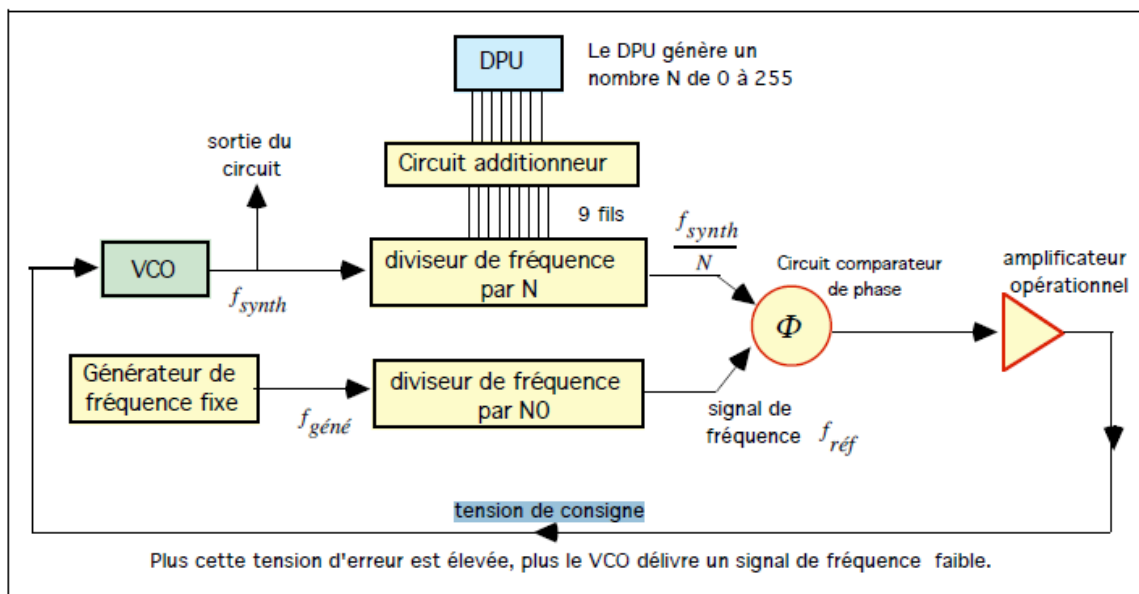


Fig. Frequency synthesizer circuit

This circuit is composed of a Phase Lock Loop (PLL), digitally controlled [KNO79], [POI92], [CNE94]:

The VCO synthesizes a signal at the frequency f_{synth} . The frequency of this signal is divided by a value N , by means of a frequency divider circuit. The variable value N is indicated by the DPU by means of 9 control wires to generate the 256 possibilities, through an adder circuit: digitally controlled division chain. On the other hand, a fixed frequency generator provides a frequency signal f_{gene} . By means of a frequency divider circuit (with a given value $N0$), a reference frequency signal f_{ref} is obtained. The frequencies f_{ref} and f_{synth} are then compared by means of a phase comparator circuit: the output voltage of the phase comparator circuit is proportional to the phase shift between these two signals, and constitutes the error signal of the control loop. This error voltage is amplified by an operational amplifier, thus generating a setpoint voltage which controls, by feedback, the VCO (analog servo).

The phase comparator circuit requires that, in the steady state of the control loop, we have:

$$\frac{f_{synth}}{N} = f_{ref}$$

For RAD1: $f_{ref} = 4 \text{ kHz}$ (frequency increment), so:

$$f_{synth} = N \cdot 4 \text{ kHz}$$

For RAD2: : $f_{ref} = 50 \text{ kHz}$ (frequency increment), so:

$$f_{synth} = N \cdot 50 \text{ kHz}$$

3.3.2. Signal transposition

To make the desired frequency range (see next §), we have:

For RAD1 :

Minimum value of N :	$N_{min} = 2676$ i.e.,	$f_{synth} = 10.704 \text{ MHz}$
Maximum value of N :	$N_{max} = 2931$ i.e.,	$f_{synth} = 11.724 \text{ MHz}$

For RAD2:

Minimum value of N :	$N_{min} = 450$ i.e.,	$f_{synth} = 22.5 \text{ MHz}$
Maximum value of N :	$N_{max} = 705$ i.e.,	$f_{synth} = 35.25 \text{ MHz}$

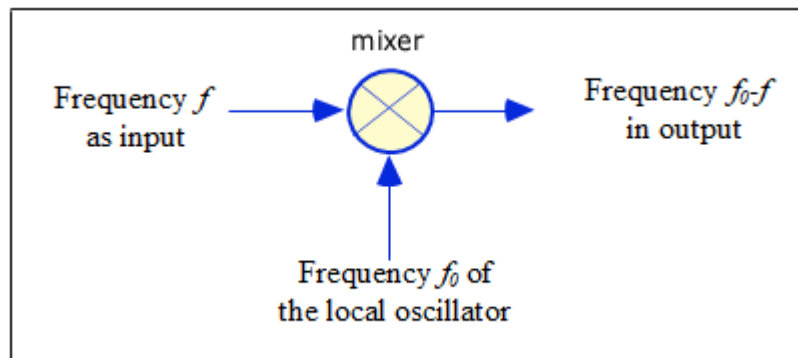
- By mixing with the signal of frequency f_0 generated by the VCO, the input signal, included in the frequency range $[f_{min}, f_{max}]$, is thus transposed in frequency in a range $[f_0 - f_{max}, f_0 - f_{min}]$.
- The electrical oscillations generated in the antenna are superimposed, after low-noise amplification, on those of a local oscillator to give rise to oscillations of a constant frequency which can be easily amplified and filtered.

We have the following table:

	RAD1	RAD2
Frequency of VCO f_0	From 10,704 MHz to 11,724 MHz	From 22,500 MHz to 35,250 MHz
Input frequency f	From 0,020 MHz to 1,040 MHz	From 1,075 MHz to 13,825 MHz
Resulting frequency in exit $f_0 - f$	10,684 MHz	21,425 MHz

3.3.3. Selective filtering - Second frequency transposition

A local oscillator (L.O.) -see operation [CNE94] p. 75- transposes the signal again by mixing:



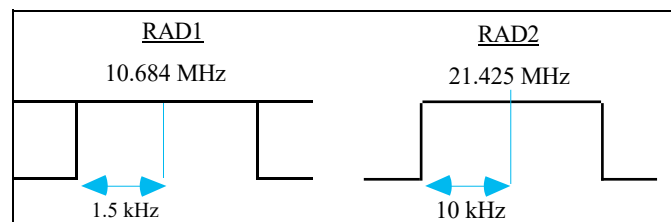
We have the following table:

	RAD1	RAD2
Local frequency oscillator	10,600 MHz	21.300 MHz
Input frequency	10.684 MHz	21.425 MHz
Frequency after mixing	$10,684 - 10,600 = 84$ kHz	$21,425 - 21,300 = 125$ kHz

- A crystal filter with a central frequency¹² of 10.684 MHz for RAD1 and 21.425 MHz for RAD2, and a very precise bandwidth (3 kHz for RAD1 and 20 kHz for RAD2) selects a small part of the spectrum corresponding to the input signal to:

$$\text{RAD1: } f_0 - 10.684 \pm 1.5 \text{ kHz.}$$

$$\text{RAD2: } f_0 - 21.425 \pm 10 \text{ kHz.}$$



¹² The intermediate frequency is chosen high enough that the $1/f$ noise of the mixer is neglected. The frequency change brings the signal into the frequency domain where it can be more easily manipulated (amplified, filtered).

The frequencies at the mixers are as follows:

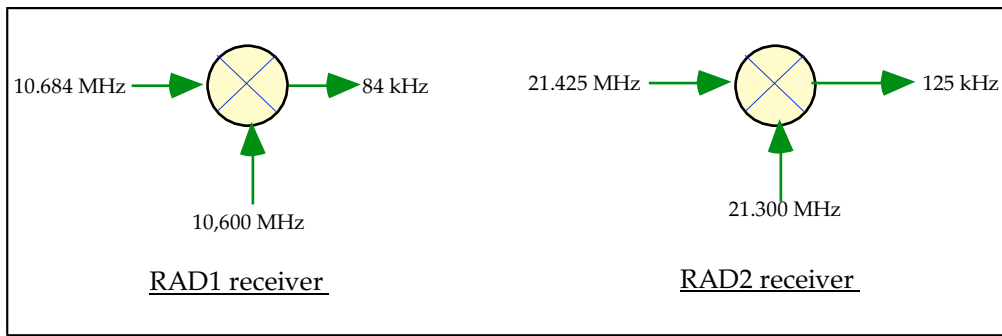


Fig. Frequencies at the RAD1/2 mixers

3.3.4. Phase shifters

We use 45° phase shifters because it is not possible in practice to realize a 90° phase shift exactly, which would correspond to the theoretical case of a pure capacitor. We have the following diagram:

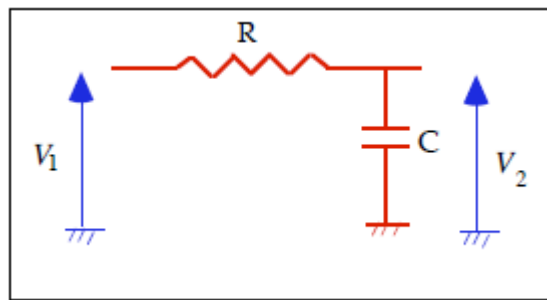


Fig. Phase shifter

We can therefore write:

$$\frac{V_2}{V_1} = \frac{1}{jC\omega \left(R + \frac{1}{jC\omega} \right)} = \frac{1}{1 + RC\omega j} R$$

For the condition $RC\omega = 1$, we have:

$$\frac{V_2}{V_1} = \frac{1}{2} - \frac{1}{2}j = \frac{1}{\sqrt{2}} e^{-j\frac{\pi}{4}}$$

This results in a phase shift of -45° between V_1 and V_2 .

When we have:

-45° on the lower part of the Z channel, we have a phase shift of: $-45^\circ - (-45^\circ) = 0^\circ$.

+45° on the lower part of the Z channel, we have a phase shift of: $+45^\circ - (-45^\circ) = 90^\circ$.

3.3.5. Automatic gain control

The automatic gain control¹³ (AGC) circuitry maintains a constant power level and avoids saturation at the input of the signal processing stages, even for significant variations in the input signal. This is necessary because of the very high dynamic range required by the signals, including the possibility of intense events. A variable gain amplifier is used for this purpose: the gain is adapted by feedback to the input signal amplitude. After detection (measurement of the RMS value), the output signal of the amplifier always has the same RMS value. This allows a good gain stability and a high dynamic range without the need for gain switching systems.

Note that, unlike the TNR, only the "AGC voltage" is retained at the output of this circuit: the fluctuating signal before detection is not taken into account.

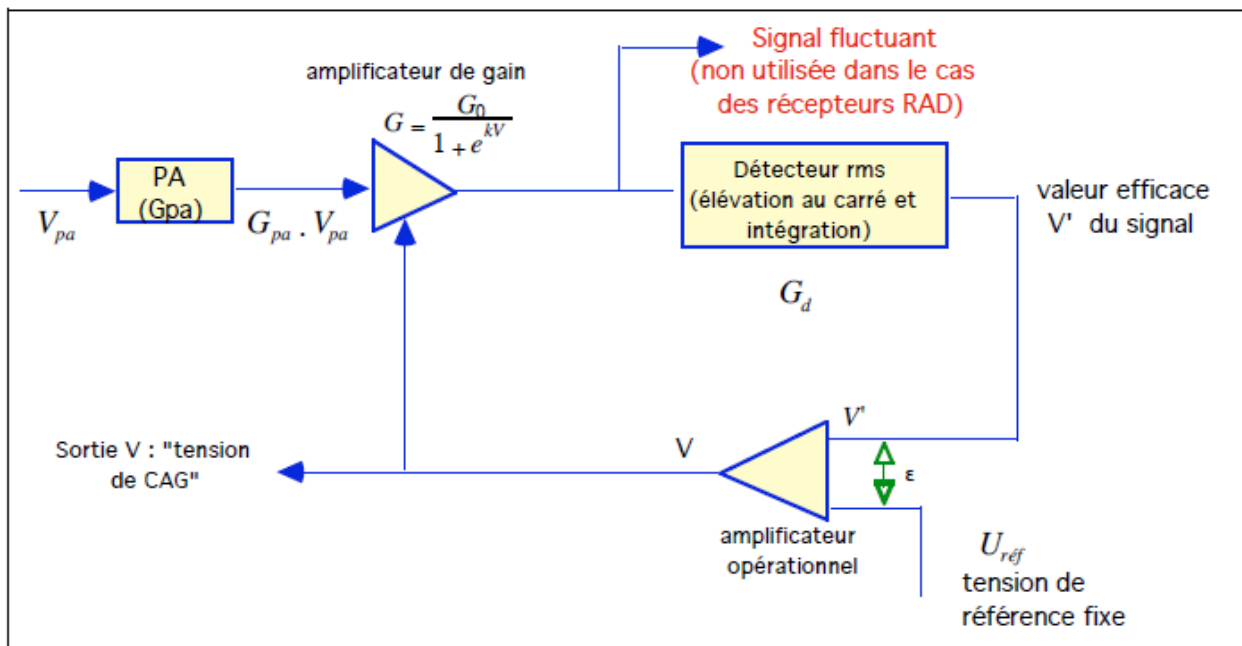


Fig. Automatic gain control

The purpose of this circuit [CAR] is to provide an output signal whose RMS value V' is a constant, whatever the amplitude level of the input signal (normalization of the receiver input to an optimal value). This value V' will be proportional to the noise energy measured in the passband of the filter of the considered channel.

To do this, the comparator (operational amplifier of theoretically infinite gain, in practice of very large gain to amplify the error) must supply at its output a voltage V which is such that V' is constant and is equal to U_{ref} at the equilibrium state of the comparator. Now V' can be written:

$$V' = (G_{pa} \cdot G \cdot G_d) V_{pa} \cdot$$

Considering the expression of the gain of the amplifier (logarithmic: its gain varies in the opposite direction of the control voltage V , according to an exponential law):

¹³ Automatic Gain Control (AGC).

$$V' = \left(G_{pa} \cdot \frac{G_0}{1 + e^{kV}} \cdot G_d \right) V_{pa} = U_{réf}$$

so:

$$V = \frac{1}{k} \text{Log} \left(\frac{V_{pa}}{V_0} - 1 \right)$$

with:

$$V_0 = \frac{U_{réf}}{G_{pa} G_0 G_d}$$

The voltage V is called the AGC voltage (or value): it controls the gain G of the amplifier and represents the total power in the band.

The logarithmic amplifier is a double transistor circuit: its operating principle takes advantage of the exponential relationship that links the current of a transistor to its emitter voltage.

Note: the non-linear analog servo problem of the AGC circuit must be mathematically translated into a system of non-linear differential equations, and is not completely solved in the literature. As is usual in such cases, the solution is approached by "linearizing" the equations or by simulation [ROH, MER81].

3.3.6. Analog-to-digital conversion

The rest of the circuit is as follows: for each of the S and Z channels, the voltage V corresponding to the stabilization gain of the AGC amplifier is converted into a square-wave digital signal, with a frequency proportional to V : this is an analogue-digital conversion by voltage/frequency conversion. The DPU periodically sends an integration control signal: as long as this signal is high, a counter included in an integrated circuit counts the number of periods of this signal. The corresponding digital values S, S' and Z are transmitted to the DPU, via a shift register, as shown in the diagram below.

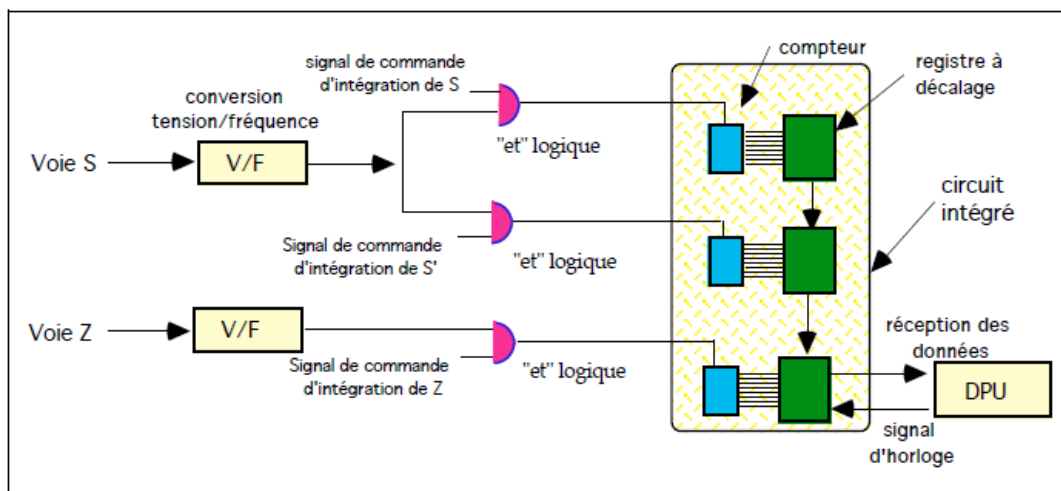


Fig. Schematic diagram of the timing circuit

The time diagram corresponding to the above diagram is as follows:

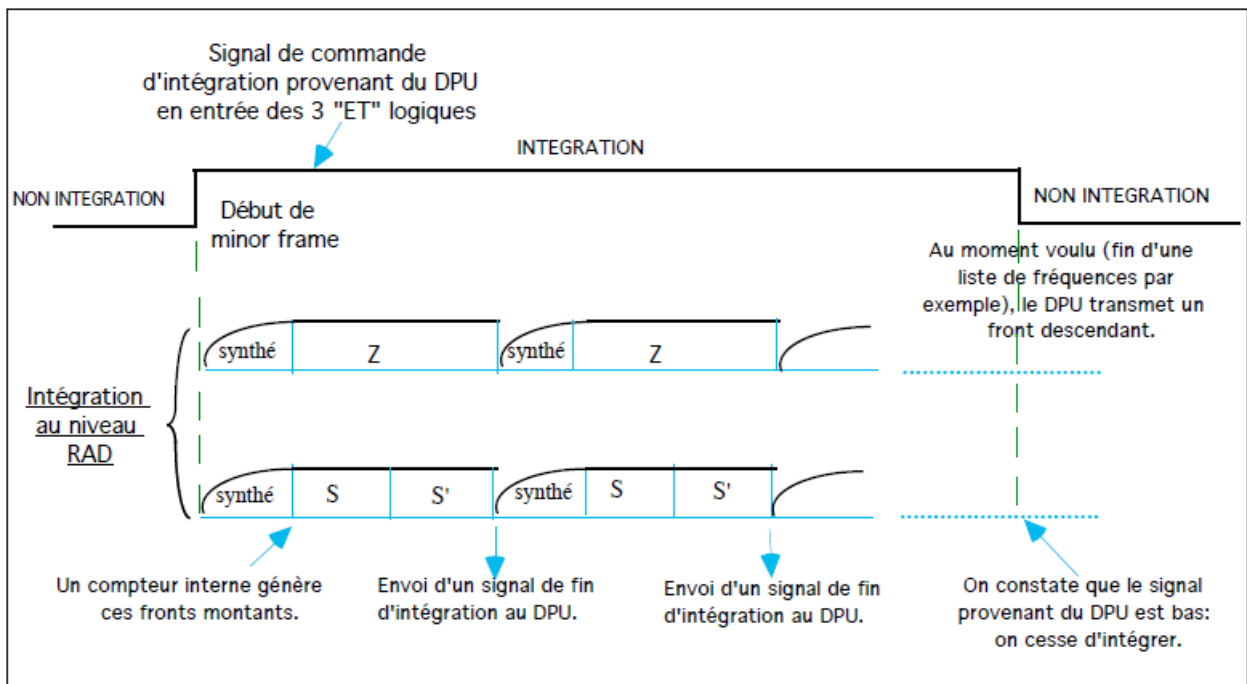


Fig. Time diagram

During synthesizer stabilization, the DPU must perform the following operations: transfer (from counter to shift register), reset, send data to the DPU one after the other, change frequencies.

Remark:

This integration technique, performed here digitally, improves the analog integration performed with an operational amplifier (O.A.), as in the ULYSSE/URAP experiment. We had then a ramp integrator: constant current loading of a capacitor. The integration was called perfect because it did not depend on the charge time constant of the capacitor.

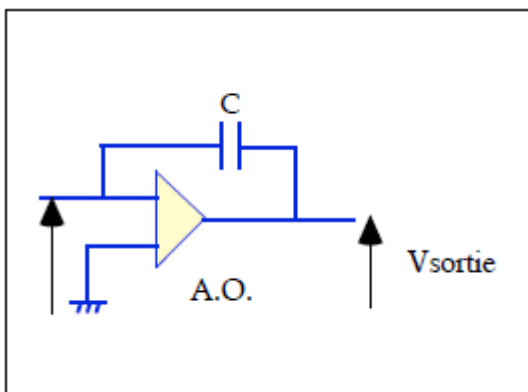


Fig. "perfect" integrator

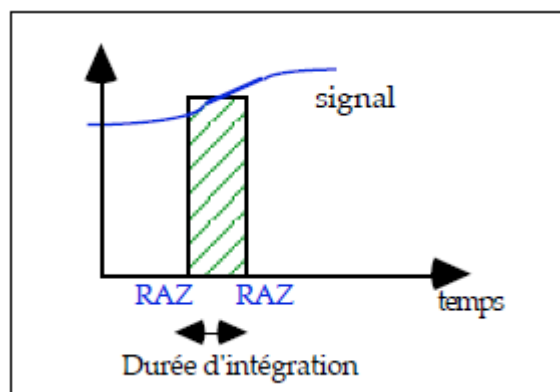


Fig. signal integration

The digital component used here avoids the disadvantages (leakage) associated with the analog circuit.

RAD1/2 Receiver Summary Features

	RAD1	RAD2
Possible inputs	Ex, Ey, Ex+Ez, Ey+Ez, Ez	Ey, Ey+Ez, Ez
Frequency range	20 kHz - 1040 kHz	1.075 MHz - 13.825 MHz
Number of frequencies	256	256
Frequency increment	4 kHz	50 kHz
Bandwidth at 3 dB (S or Z channel filter)	3 kHz	20 kHz
Dynamic range	approx. 70-80 dB	approx. 70 dB
Frequency	10,684 MHz	21,425 MHz
Frequency of the 2nd O. L.	10,600 MHz	21,300 MHz
Fluctuations	0.2 dB	0,24 dB
Equivalent noise bandwidth (filter channel S)	3,48 kHz	19 kHz (to be refined)
Equivalent noise bandwidth (filter channel Z)	3,37 kHz	19 kHz (to be refined)

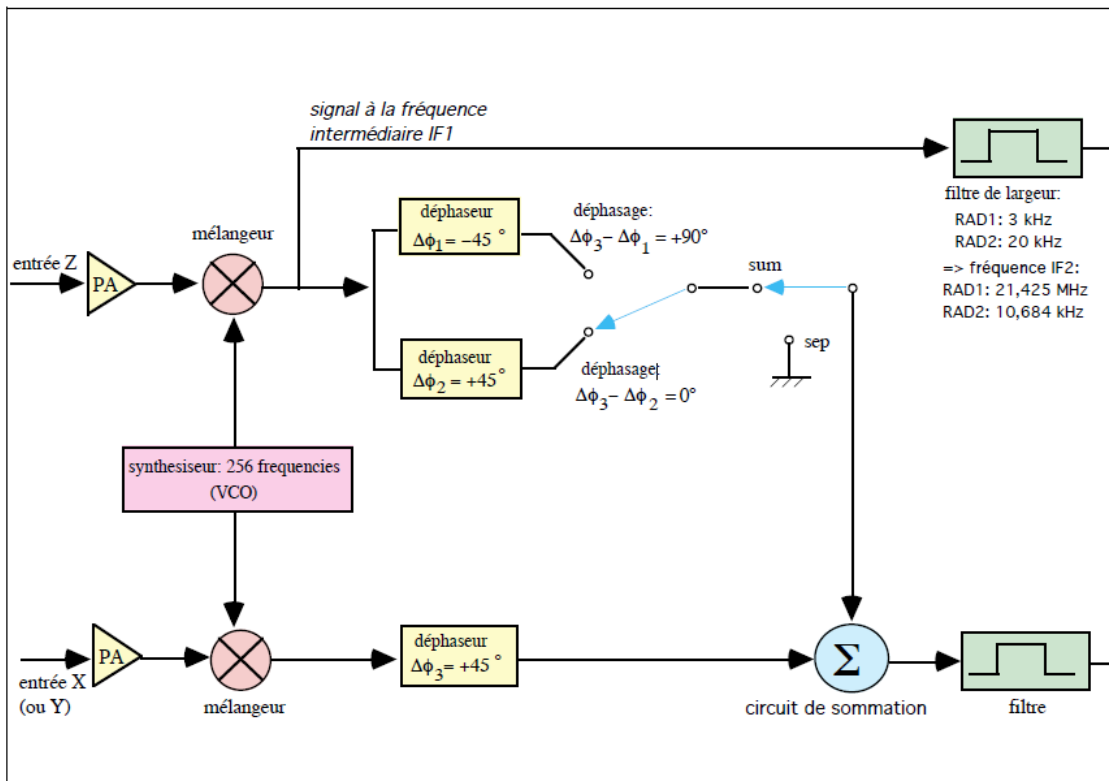


Fig. Block diagram of RAD1/2 receivers

3.4. Direction and polarization of sources: synthetic dipole technique

3.4.1. General principle

The direction of a radio source (direction of the wave vector k of the electromagnetic wave) can be characterized by the two angular quantities azimuth and elevation:

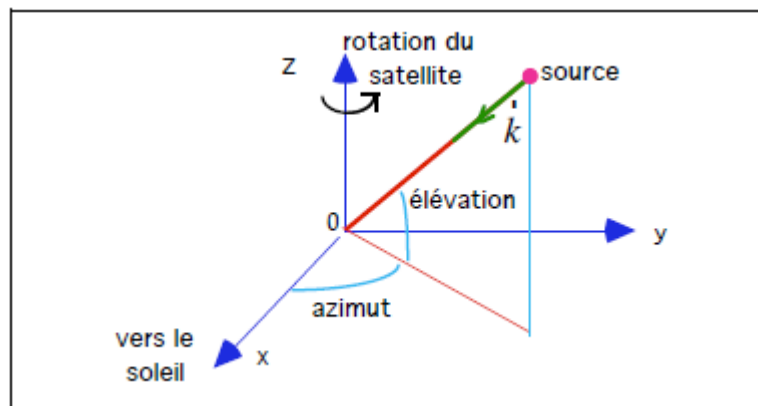


Fig. Parameters characterizing the direction of a radio source

If the radio source is not considered to be a point source, its angular half-width is also considered.

To measure this direction, the properties of an electrically short dipole are used. The radiation pattern of a dipole cancels along its axis. During the rotation of the satellite, the main radiation lobe of the antenna sweeps over the source region, resulting in a time signal with a profile modulated by the rotation of the satellite: "spin modulation".

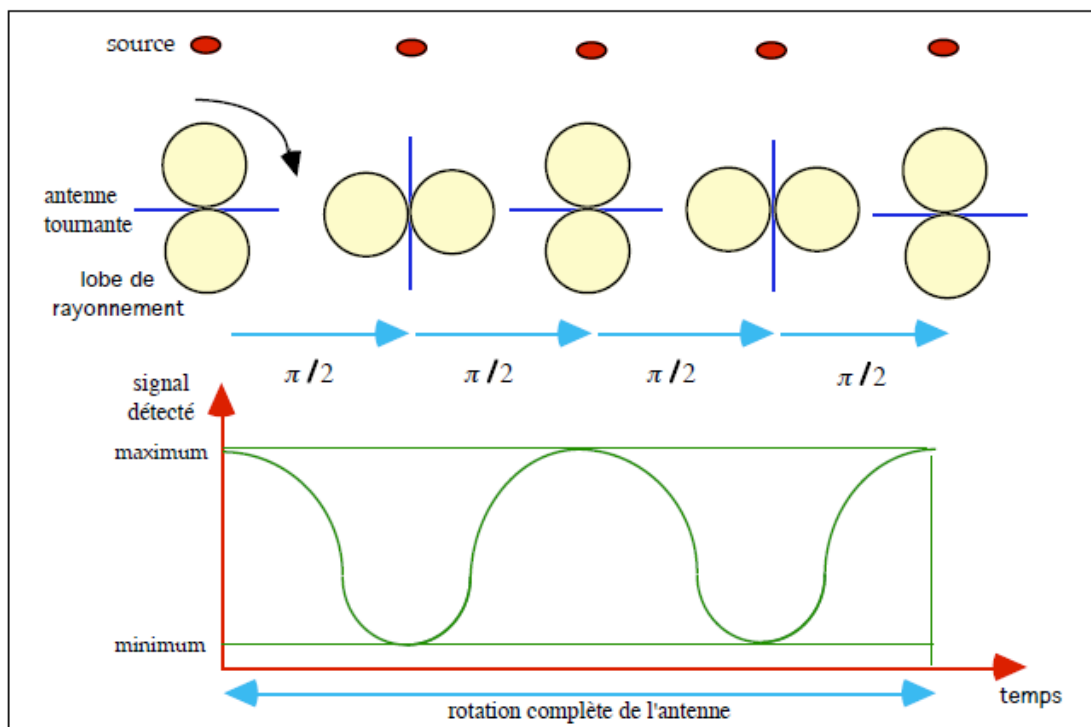


Fig. Evolution of the signal with the rotation of the antenna

When the axis of the dipole is pointed towards the source, a minimum signal is observed. Conversely, when the source is located on the axis of the dipole, a maximum signal is collected. The ratio between the maximum and the minimum is all the more pronounced as the angular extent of the source is low. The amplitude minima will only be zero when the source is occasionally located in the rotation plane of the antenna.

The modulation index can be defined:

$$\alpha = \frac{I_{\max} - I_{\min}}{I_{\max} + I_{\min}}$$

I_{\max} and I_{\min} are the maximum and minimum signal strength respectively. The modulation index is between 0 and 1. The modulation index is close to 0 for a wide source, and close to 1 for a narrow source.

By analyzing this modulation imposed by the rotation of the probe, the direction of the radio source can be determined. The precise determination of the phase of the amplitude minima with respect to the rotation cycle makes it possible to deduce the azimuth of the source¹⁴. Note that the signal received by the E_z antenna is not modulated in principle (except when it is tilted [FAI]).

3.4.2. The Mathematical Method

3.4.2.1. Principle

In the case of a source assumed with a uniform circular distribution, and partially polarized, a mathematical method has been developed [MAN80] for a spinning satellite, allowing to determine the different physical parameters: direction of the "centroid" (azimuth and elevation) and angular half-width of the source, and also polarization, characterized by the four Stokes parameters. We report here the essential conclusions in order to introduce the notions necessary for the understanding of the instrument. We invite the reader to refer to the two basic publications [MAN80] and [FAI85] for the detailed calculations.

The polarization of the incident wave is described synthetically by the four Stokes parameters¹⁵ : U, V, Q, S . It should be noted that the absence of a possible polarization in the calculations can lead to errors of appreciation in the direction of the sources. For some radio emissions such as type III bursts, direction finding alone may be sufficient. For other sources such as terrestrial¹⁶ or Jovian bursts, it is important to take into account the polarization data [LEC].

To describe the direction of the source, the following angular quantities are considered:

θ : polar angle (complementary angle to 90° of the elevation: polar angle = 90° - elevation).

γ : half angular width of the source, assumed to be conical.

ϕ : azimuth of the center of the probe.

It is shown that the output powers of the S-channel and the Z-channel are written as

¹⁴ In the general case of a source that is not in the plane of rotation of the antenna, the phase of the minima can still be used to deduce the azimuth, but their depth is a function of both the elevation and the angular diameter of the source (and the S/N ratio).

¹⁵ Cf. glossary. This formalism is common in radio astronomy where the sources are not fully polarized (partially polarized sources): the amplitudes and phases of astrophysical waves generally vary with time.

¹⁶ However, AKR bursts, due to their rapid evolution, are more difficult to analyze in terms of direction and polarization.

$$P_{syn}(t) = G_0 Z_0 S \left[P_0 + P_1 \cos(\omega t - \phi) + P_1' \sin(\omega t - \phi) + P_2 \cos 2(\omega t - \phi) + P_2' \sin 2(\omega t - \phi) \right]$$

$$P_z(t) = G_0 Z_0 S(P_0)_{R=0}$$

With:

ω : speed of rotation of the probe.

G_0 : total system gain.

Z_0 : intrinsic impedance of the vacuum. $Z_0 = 120\pi \Omega$.

S : absolute or measured density flux over the radio emission region.

The coefficients P_i and P_i' depend on the Stokes coefficients U , V , Q , and R (see § 5), δ , θ , and γ . The quantities R , G_0 , and δ assumed to be known, 7 parameters remain to be determined: the angular parameters characterizing the direction (ϕ , θ , γ) and the intensity and polarization parameters (S , U , V , Q).

From Fourier analysis of the rotation-modulated signal obtained by summing, alternately in phase and in quadrature, the outputs of the equatorial and axial antennas, shows that only 6 equations are available [MAN80]. However, we notice that for $\delta = 0^\circ$, the circular polarization parameter V disappears from the equations. By using alternately $\delta = 0^\circ$ and $\delta = 90^\circ$, the parameter V can also be calculated. This explains the hardware design of the RAD1/2 radio receivers (or RAR receivers of similar design, in the framework of the ULYSSE/URAP mission). Exact analytical expressions could be obtained for the parameters to be determined. However, it is preferred to use an iterative numerical non-linear optimization procedure (non-linear least squares method) with fitting using 7 parameters.

For one rotation of the probe, we use:

- n_1 measures m_i^1 of the synthetic track with $\delta = 0^\circ$ (S measurements).
- n_2 measures m_i^2 of the synthetic track with $\delta = 90^\circ$ (S' measurements).
- n_3 measures m_i^3 of the Z track (Z measurements).

We are looking for the set of 7 parameters noted Q_j that minimize the sum of the three terms:

$$D = \sum \left(m_i^1 - P_{synth}(Q_j, \delta = 0^\circ, t_i) \right) +$$

$$\sum \left(m_i^2 - P_{synth}(Q_j, \delta = 90^\circ, t_i) \right) +$$

$$\sum \left(m_i^3 - P_z(Q_j, t_i) \right)$$

The summations are for the n_1 , n_2 , n_3 measurements respectively.

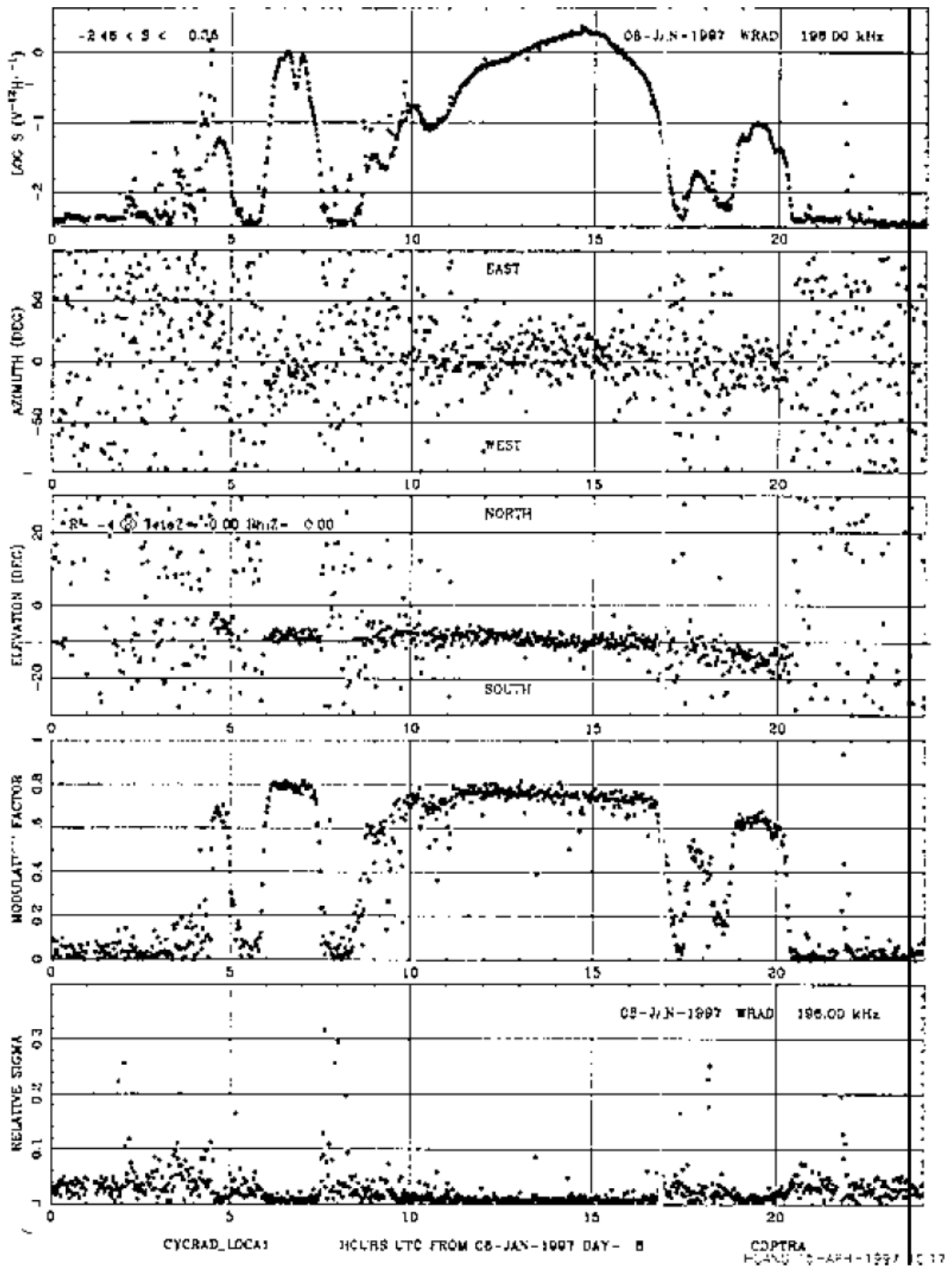
Using 8 measurements per satellite rotation, the root mean square error obtained in this way is less than 1° for the determination of the direction parameters, and typically of the order of 1-10% for the determination of the polarization parameters. A reliable direction measurement obviously assumes that the source intensity varies slowly over a period of probe rotation.

This method was later extended [FAI85] to take into account a possible tilt of the antenna with respect to the Z-axis resulting from mechanical misalignment, or from an offset of the electrical axis of the dipole due to parasitic currents in the structures surrounding the satellite. The mathematical method implemented is based on the same considerations, with three additional parameters to describe the axis tilt. In particular, the equations giving P_{syn} and P_z are the same; only the expressions of the parameters P_i and P'_i change.

The shorter axial antennas are more subject to such tilts. This effect can become important when considering a monopole antenna, as on the Ulysses probe, where a symmetry defect in the satellite body can cause a tilt of the electrical axis. The calculation of the electrical tilt for the dipole antenna of the ISEE3 probe led to a very low value ($< 1^\circ$).

The diagram on the next page shows the intensity (in $\mu V \cdot Hz^{-1/2}$), the azimuth and the colatitude of the source, as well as the modulation index α .

The applications of this method are in particular the mapping of the interplanetary magnetic field, the detection of Jovian bursts, the detection of type III radio bursts associated with Langmuir waves (see appendices).



3.4.2.2. Physical implementation

For a complete measurement of the polarization of the incident wave, more precisely the parameter V , which describes the circularly polarized component of the wave, we have seen that we must artificially introduce a phase shift between the signal received at the E_z antenna and the signal received at the E_x or E_y antenna. This is achieved by means of phase shifters (see diagram § 3-3-4). The phase shift determines the ellipticity of the antenna polarization.

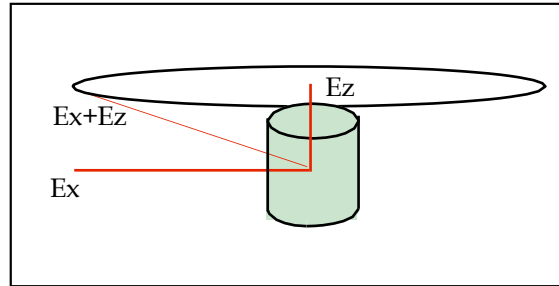


Fig. Inclined synthetic dipole (case of zero phase shift between S and Z channels)

The SUM and SEP modes for the RAD1/2 receivers correspond respectively to the activation or non-activation of the synthetic tilted dipole synthesis. The dipole synthesis method consists in summing¹⁷ (SUM mode) the signals from the E_x (or E_y) and E_z antennas. S and S' are noted respectively:

	Mode	Phase difference between channels Z and (X or Y)
S	SUM: (X or Y) + Z	$\delta = 0^\circ$
S'	“ “	$\delta = 90^\circ$ ¹⁸

In the mode for which the synthesis of the channels (X or Y) and Z is not performed (separate mode or SEP mode), the outputs S and S' are approximately equivalent (except for calibration measurements, because the electronic circuit is slightly different, and crosstalk phenomena may occur).

The sensitivity increases with the length of the antenna¹⁹: the direction of the source is therefore determined with greater accuracy by summing the channels (E_x or E_y) and E_z . On the other hand, the gain of the preamplifier of the axial antenna should be smaller than that of the equatorial antennas, since a synthetic dipole should be tilted at about 30° . Since the background noise is determined by the shorter antenna²⁰ (here E_z), however, the noise level is also increased in this way. Similar techniques have been used for the ISEE3/ICE and ULYSSE/URAP experiments [STO92,STO83].

A "Polar Inhibit" command is available to inhibit the summation alternatively with and without phase shift, in case the corresponding results are unusable.

¹⁷ The addition is done at the output of the first mixer, in order to realize this addition at constant frequency. This is due in particular to the fact that a functional adder cannot be realized for a whole frequency range.

¹⁸ Or 0° possible ==> $S = S'$, see command "Polar Inhibit", later in the text.

¹⁹ This sensitivity varies as about L^2 to L^4 , where L is the length of the antenna.

²⁰ For the same noise level, the longer the antenna, the higher the signal level and the higher the signal-to-noise ratio. It is recalled that the receiver noise is mainly due to the preamplifier.

3.5. Measurement acquisition RAD1/2

3.5.1. The different modes of acquisition

RAD1/RAD2 radio frequency receivers can acquire data in several modes:

The "linear sweep mode"

Linear sweep operation is used to observe slowly changing phenomena and to analyse possible noise and interference. It is also used for ground testing. The receiver scans a list of contiguous frequencies in ascending frequency order. *The number of frequencies scanned in this mode is specified by remote control: it is usually 256, with a frequency increment that is specified, the first frequency being programmable.*

The "list sweep" mode

The purpose of the list sweep mode, also called normal mode, or measurement mode, is the complete characterization of the radio source parameters: intensity, direction, angular diameter, polarization. The frequencies in this mode are selected from the 256 frequencies of the line sweep mode. The order of scanning frequencies is determined by selecting a list of frequencies and a table of pointers to these frequencies. The pointer table is scanned according to an algorithm specified in § 3-5-3-1. The sweep continues until another list of frequencies is selected by remote control.

The intensity time profile of a Type III burst, the main event sought by RAD1/2 receivers, is similar in shape at all frequencies, but its duration is (approximately) inversely proportional to the frequency. Therefore, for optimal resolution of these events, high frequencies must be measured more often than low frequencies. This results in a non-linear frequency sweep.

To fully characterize the source, a minimum number of samples must be acquired during one rotation of the probe at each observation frequency in order to reconstruct the signal modulation²¹. In the case where one only wishes to analyse an event without taking into account the intensity modulation aspects due to the rotation, one could, for example, take, at each rotation, the maximum of the readings, which gives the maximum intensity of the source.

The "fixed frequency" mode

The receivers are positioned on a fixed frequency ("freeze" or "fixed tune" mode) which can be selected from the 256 frequencies of the "linear scan" mode. The purpose of this mode is the detailed analysis of disturbances or particular phenomena at fixed frequency. It is thus possible to obtain very high time resolution data at a given frequency. An event will contain 256 samples (S, S', Z). This mode, except shortly after launch, has not been implemented so far.

The "internal calibration" mode

In flight, the response curve of the receivers is susceptible to more or less perceptible variations due to the space environment and the electronic components. In the internal calibration mode, calibration sequences ("CAL sequences") are periodically applied to the receivers, using a calibrated noise generator, internal to the experiment. In this way, the evolution of the response curves of the receivers. A drift detection is eventually followed by a ground update of the calibration parameters of these curves (see calibration chapter).

²¹ These issues will be developed in the following paragraphs.

We have the following constants:

Item name	Definition	Duration in ms RAD1	Duration in ms RAD2
START_OFFSET_SPRIME_R4	time between the beginning of the event and the first measurement S'	50 + 154	204
START_OFFSET_ZS_R4	time between the start of the event and the first measurement S or Z	50	23
OFFSET_TO_NEXT_SET_R4	Time between 2 measurements of (S, S', Z)	358	63
OFFSET WITHIN SET R4	?	0	0
INTEGRATION TIME S R4	integration time of item S (or S')	154	20
INTEGRATION TIME Z R4	integration time of the item Z	308	40

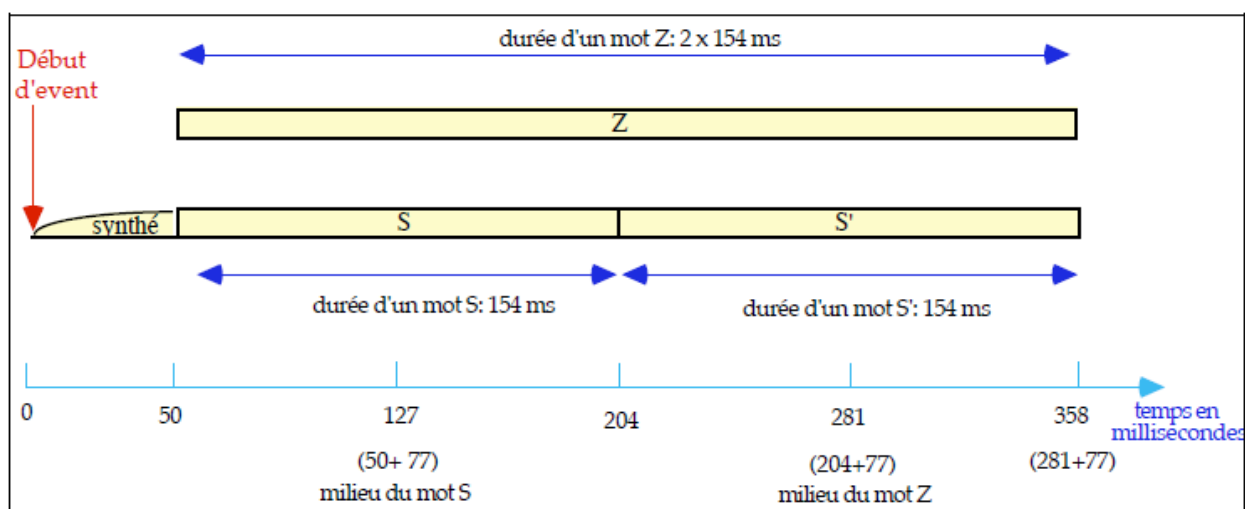
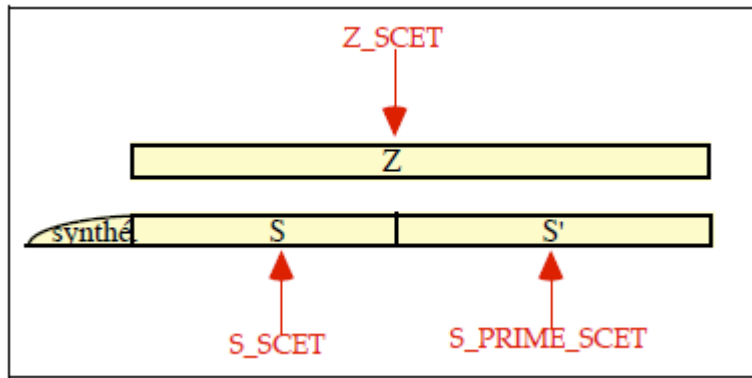


fig Measurement times - RAD1 receiver

The event start time is given by the "item": EVENT_SCET_R8

Remarks :

- The times S_SCET, S_PRIME_SCET and Z_SCET given by the WIND software library, associated respectively to the S, S' and Z measurements, correspond to the middle of the measurement; they are thus directly corrected for the integration effect:



- The times provided by the WIND/Waves library are already corrected by a factor that accounts for the fact that the times *measured* by the Waves experiment are based on the internal clock of the DPU, which may vary slightly around the nominal 50 Hz value. *This corresponds to the item DPU_CLOCK (TBV).*

- K. Goetz plans to implement the satellite angular position information for each S, S' and Z item.

3.5.2. Linear sweep mode

In linear sweep mode, the measurement time for a frequency corresponds to the cumulative duration of the synthesizer rise times and the acquisition times of the S, S' and Z words, as shown in the following diagram:

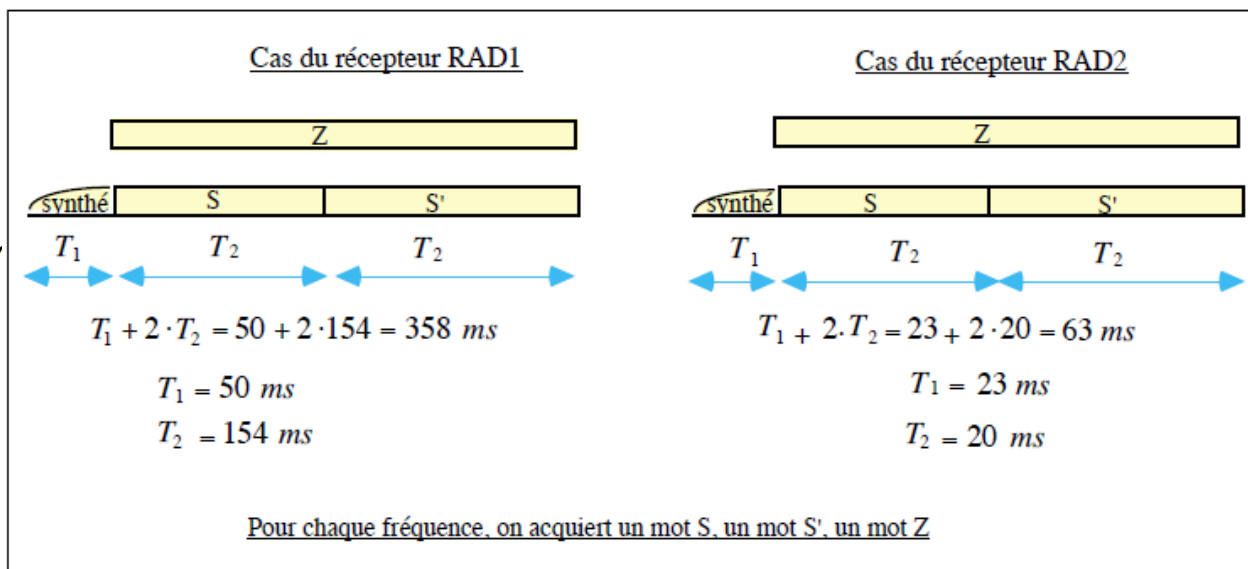


Fig. measurement times RAD1/2

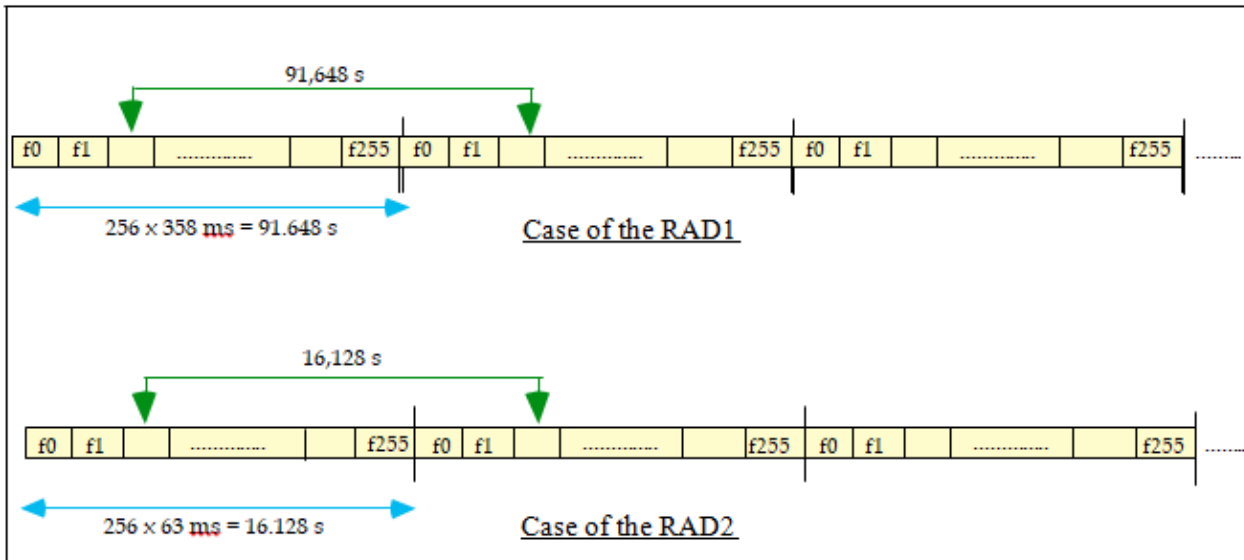
Remarks

- The acquisition of the Z word is concomitant with that of the S and S' words: the Z signal, which is not very modulated compared to the S and S' signals, is sampled less often.
- The times shown are related to the instrument electronics and are the same for the list sweep mode.

A line sweep event contains 256 samples. The time required to obtain 256 samples is:

Case RAD1: 358 ms x 256 = **91,648 s**

Case RAD2: 63 ms x 256 = **16,128 s**



The "items" of the WIND/Waves software library specific to this mode are:

- FIRST_FREQ_NUM: number of the first sweep frequency.
- LAST_FREQ_NUM: number of the last sweep frequency.
- FREQUENCY_STEP: interval between each measurement.
- CHANNEL_NUMBERS: frequency numbers.

By only running the 256 frequencies in one event in the form of 4 series of 64 frequencies, at the cost of a loss in frequency resolution, we gain in temporal resolution.

Case RAD1: 358 ms x 64 = **22,912 s**

Case RAD2: 63 ms x 64 = **4,032 s**

The frequency numbers range from 1 to 253, for example, with 4 frequency channels in between:

- FIRST_FREQ_NUM: 1
- LAST_FREQ_NUM: 253
- FREQUENCY_STEP: 4

frequency numbers in the event:

1	5	9	13	245	249	253
1	5	9	13	245	249	253
1	5	9	13	245	249	253
1	5	9	13	245	249	253

Remarks:

- The choice of list mode or linear sweep mode data acquisition can be tricky, as it depends on the events to be studied. While the linear sweep mode leads to a high frequency resolution, the time resolution is critical: it takes about 16 seconds (RAD2) and one and a half minutes (RAD1) to find the same frequency. For example, to obtain 8 samples at the same frequency, it will take $8 \times 1.5 = 12$ minutes (RAD1) in linear sweep mode, whereas in list mode these 8 samples are obtained in a complete measurement cycle of 3 minutes (if we consider the highest frequencies for example).
- This mode is more adapted to the study of planetary emissions (terrestrial or Jovian for example). It does not allow to consider efficiently a study of type III bursts and in particular the direction of the emitting sources for which the list mode offers a much better temporal resolution.
- Note however that a high temporal resolution constitutes an advantage for the analysis of planetary emissions and it appears for example that the LF (Low Frequency events) bursts, discovered within the framework of the ISEE3 mission for the first time [STE88], and which one also studies through the WAVES data, rather require the list mode. Finally, we recall that the measurement of the direction of the sources, which varies little, is possible in line sweep mode where the modulation of the sources can be observed. Such a study has already been conducted in the past [].
- To date, both options have been remotely controlled, with a clear predominance of the list mode. The line sweep mode is implemented two days per month.

3.5.3. The list sweep mode

3.5.3.1. Scheduling algorithm

In normal mode, during a measurement cycle, the probe performs several rotations. For each step corresponding to approximately one rotation, and for a given number of frequencies, samples S, S' and Z are collected.

Receiver sweeping²² is controlled by the selection of:

- A list of frequencies from the available lists.
- A table showing the order of frequencies to be scanned in this list.

This indirection process has the advantage of allowing the synthesis of a large number of frequency lists.

²² The Waves packet header contains list number and table number information.

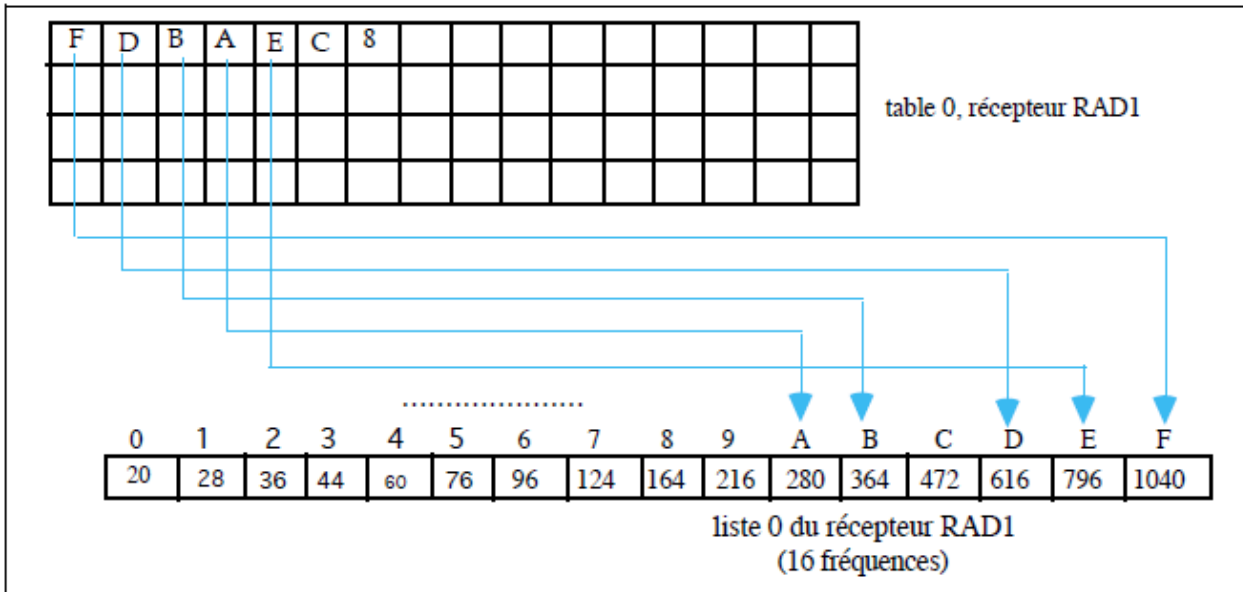


Fig. addressing the frequencies of a list

The measurement scheduling algorithm for RAD1 or RAD2 receivers is as follows:

```

Do for i = 1, N
  Do for l = 1, y (To be confirmed)
    Do for j = 1, M
      Do for k = 1, P
        Read the following pointer in the current table
        Deduce the frequency pointed to in the frequency list in force
        Acquire S, S' and Z for this frequency
      End do
      Go to the next group of P pointers
    Do End
  Do End
Do End

```

The symbols have the following meaning:

SYMBOLE	SIGNIFICANCE	ASSOCIATED ITEM (WIND software library)
N	Number of steps (rotations) per measurement cycle	STEPS
M	Number of times the group of pointers of the table is taken into account in a step.	GROUP_LOOP
P	Number of elements in the pointer group.	GROUP_SIZE
y	1: always in SUM or SEP mode 2: alternation (SUM rotation - SEP rotation)	SUM_LOOP (tbc)

- The total number of entries in a table is equal to $N \times P$. This is the number of frequencies scanned during a measurement cycle.

$$\text{For RAD1: } N \times P=64$$

$$\text{For RAD2: } N \times P=48$$

- The option $y = 2$, which consists in alternating (rotation in SUM mode) / (rotation in SEP mode), gives additional points and thus allows a better determination of the direction of the sources. It seems that this option has not been implemented in the pointer tables (see § 3-5-3-6-1 and 3-5-3-6-1), for RAD1 as well as for RAD2 (y is always 1). There is still a possibility of downloading (TBC).

SUM/SEP: toggle: TBC - Alternate SUM/SEP

3.5.3.2. Examples

For example, consider the RAD1 receiver. There is a table with 64 entries, each representing a frequency number. The pointer tables are read from left to right and from top to bottom. Consider the case of table 0 (§ 3-5-3-6-1) and list 0 (§ 3-5-3-9). The table indicates the succession:

F D B A E C 8 7 F D B 9 etc...

Therefore, given the scheduling algorithm, we will have the following sequence:

1040 1040 1040 1040 1040 1040 1040 1040 1040 1040 616 616 616 616 616 616 616 616 364 364 ... etc...

In the case of RAD2, if we take the example of table 0 and list 0, we have the succession:

F D 9 E C 7 F B 5 E A 3 F D 8
 E C 6
 etc...

Considering the scheduling algorithm, let the following frequencies (direction of reading from left to right and from top to bottom):

1382	9825	4975	1167	8275	3525	1382	9825	4975	1167	8275	3525
5			5			5			5		
1382	9825	4975	1167	8275	3525	1382	9825	4975	1167	8275	3525
5			5			5			5		
1382	9825	4975	1167	8275	3525	1382	9825	4975	1167	8275	3525
5			5			5			5		
1382	9825	4975	1167	8275	3525	1382	9825	4975	1167	8275	3525
5			5			5			5		
1382	6975	2525	1167	5925	1175	1382	6975	2525	1167	5925	1175
5			5			5			5		
1382	6975	2525	1167	5925	1175	1382	6975	2525	1167	5925	1175
5			5			5			5		
1382	6975	2525	1167	5925	1175	1382	6975	2525	1167	5925	1175
5			5			5			5		
1382	6975	2525	1167	5925	1175	1382	6975	2525	1167	5925	1175
5			5			5			5		
1382	9825	4175	1167	8275	2975	etc	...				
5			5								

This scheduling can also be seen in the diagram in §3-5-3-7-1 (RAD1) and §3-5-3-7-2 (RAD2).

The WIND/Waves software library items specific to this mode are listed in the table on the previous page. We can also note:

FREQ_TABLE: number of the pointer table.
 XLATE_TABLE: number of the frequency list.

In this nominal case, we have :

$$8 \quad \times \quad 6 \quad \times \quad 6 \quad = \quad 384 \text{ per event for RAD2.}$$

$$8 \quad \times \quad 64 \quad = \quad 512 \text{ per event for RAD1.}$$

3.5.3.3. Number of tables and lists available

In practice, we have:

8 lists of 16 pre-programmed frequencies in PROM for RAD1, the same for RAD2.

8 other lists that can be downloaded in the RAM²³ memory during the flight (8 for RAD1, 8 for RAD2). Before the launch, these tables are filled with zeros.

²³ The limitation in memory space is mainly in terms of PROM memory, less in terms of RAM memory.

In total, for RAD1 as for RAD2, we have a set of $8 + 8 = 16$ lists of 16 frequencies (8 in RAM, 8 in PROM).

4 pointer tables pre-programmed in PROM for RAD1 (tables with 64 entries), 6 for RAD2 (tables with 48 entries).

	RAD1	RAD2
PROM	8 lists 4 tables	8 lists 4 tables
RAM	8 lists 8 tables	8 lists # tables

3.5.3.4. Criteria for the elaboration of pointer tables

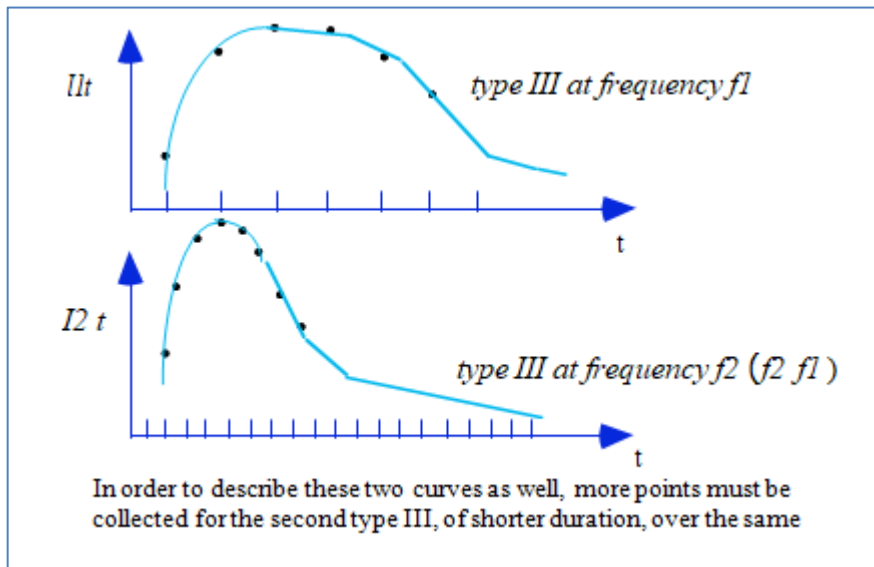
“Solar” tables

The concepts developed below are intended for the elaboration of so-called "solar survey" frequency tables²⁴. The composition of these tables reflects the following dual concern:

- As the type III generating electrons move further away from the sun, the associated emission frequency f decreases and the duration of type III bursts, $\Delta t_{typeIII}$, increases. We have the following empirical relation:

$$\Delta t_{typeIII} = \frac{220(MHz)}{f(MHz)} \text{ secondes} . \quad (1)$$

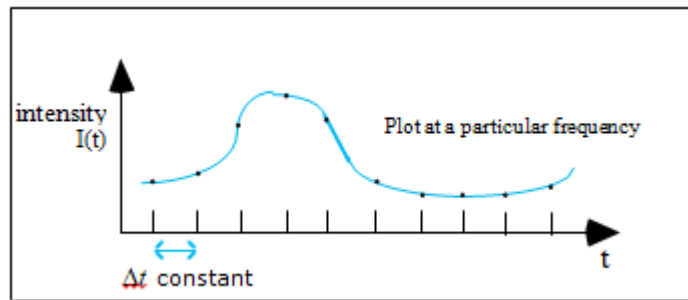
The reconstruction of the time evolution curve $I(t)$ of type III bursts requires to collect a sufficient number of points at the observed frequency during a rotation. Relation (1) shows that the different frequencies in a list should not be scanned at the same rate: in one measurement cycle, high frequencies should be scanned more often than low frequencies. As a result, the number of entries for high frequencies in the pointer table must be higher than the number of entries for low frequencies:



²⁴ The elaboration of the pointer tables and the frequency lists takes place during the period preceding the loading of the PROMs and the launching of the probe (the so-called "refurbishment" period).

Relation (1) indicates that the ratio of the durations should be approximately equal to the inverse ratio of the frequencies. In theory, therefore, $1/0.020 = 50$ times more the 1 MHz frequency should be swept than the 20 kHz frequency. Here we only have a ratio of 8:1 for the sweep of the frequency F to the frequency 0, for example for the table 0.

- For a given frequency, the measurements must be evenly distributed over time. It can be seen that the letters corresponding to the frequencies appear at regular intervals in the pointer tables. In the case of table 0, receiver RAD1, for example, there are 8 cells to go from a letter F to the next letter F.



It follows that the number of occurrences of each frequency must be a sub-multiple of $N \times P$, the total number of entries in the table, i.e. 64 for RAD1 and 48 for RAD2. This number of occurrences can therefore theoretically be 1, 2, 4, 8, 16 or 32 for RAD1, and 1, 2, 3, 4, 6, 8, 12, 16 or 24 for RAD2.

In the case of the RAD1 receiver, for example, the following system is solved:

$$a \times 16 + b \times 8 + c \times 4 + d \times 2 + e \times 1 = 64$$

(64 : total number of scanned frequencies)

$$a + b + c + d + e = 16 \text{ (because we have a list of 16 frequencies)}$$

a: number of frequencies that are scanned 16 times.

b: number of frequencies that are scanned 8 times,
etc...

This system generally admits several solutions: we choose the one that corresponds to a fairly homogeneous sweep. A possible solution is: $a = 0, b = 6, c = 2, d = 3, e = 5$. Since a frequency is scanned more often the higher its value, the 6 highest frequencies are scanned 8 times, the 2 preceding frequencies 4 times, etc...:

Frequency	0	1	2	3	4	5	6	7	8	9	A	B	C	D	E	F
Occurrences	1	1	1	1	1	2	2	2	4	4	8	8	8	8	8	8
	e = 5					d = 3			c = 2		b = 6					

“Planetary” tables

The tables for planetary survey observations are equi-swept in that the AKR and ITKR radiations fluctuate quite rapidly: the duration of the events does not depend on the frequency (TBC). One can indeed verify that for table 1, receiver RAD1, or table 1, receiver RAD2, for which the succession of letters is the same, the (numerical) interval between the letters is identical and that each letter appears 4 times (RAD1) and 3 times (RAD2).

3.5.3.5. Frequency coding

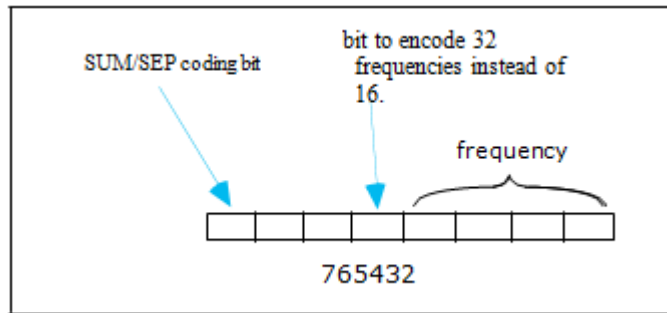
32-frequency lists

To encode 16 frequencies in a list, the use of 4 bits²⁵ is necessary. The use of an additional bit allows two *contiguous* lists (TBC) of 16 frequencies to be traversed. Bit 4 is used here. It is therefore possible to design a list of 32 frequencies, consisting of two lists of 16 frequencies. This is the case for lists 4 and 5 for RAD1 or RAD2 receivers (see § 3-5-3-9).

Sum/Sep coding

Bit #7 is used to specify whether it is a SUM or SEP mode measurement. This possibility leads to a worse resolution than alternating (SUM mode rotation)-(SEP mode rotation). Table 3 for the RAD1 receiver was designed with this in mind.

So in summary:



The frequency number, in the pointer tables, is in hexadecimal notation. We have for example:

0D:	SUM mode, frequency number 14
8D:	SEP mode, frequency number 14.
0A:	SUM mode, frequency number 10 of the low list (numbered from 0 to 15).
1A:	SUM mode, frequency number 10 of the high list (numbered from 15 to 31), i.e. frequency number 26 if we count from 0.

3.5.3.6. Pointer tables

3.5.3.6.1. RAD1 receiver

Table 0: Solar sweep, RAD1

$$0 \times \boxed{16} + 5 \times \boxed{8} + 3 \times \boxed{4} + 4 \times \boxed{2} + 4 \times \boxed{1}$$

N	y	M	P	list (default)	Sum/Sep	max. frequency no.	average over Z
64	1	8	1	0	0	15	1

0F	0D	0B	0A	0E	0C	08	07	0F	0D	0B	09	0E	0C	05	03
0F	0D	0B	0A	0E	0C	08	06	0F	0D	0B	09	0E	0C	04	02
0F	0D	0B	0A	0E	0C	08	07	0F	0D	0B	09	0E	0C	05	01
0F	0D	0B	0A	0E	0C	08	06	0F	0D	0B	09	0E	0C	04	00

²⁵ Values from 0 to 15 can be coded on 4 bits.

As this table is intended for the analysis of type III bursts, the higher frequencies are more often described.

Table 1: Planetary sweep (equi-sweep table) 16 x 4

N	y	M	P	list (default)	Sum/Sep	max. frequency no.	average over Z
64	1	8	1	1	0	15	1

0F	0B	07	03	0E	0A	06	02	0D	09	05	01	0C	08	04	00
0F	0B	07	03	0E	0A	06	02	0D	09	05	01	0C	08	04	00
0F	0B	07	03	0E	0A	06	02	0D	09	05	01	0C	08	04	00
0F	0B	07	03	0E	0A	06	02	0D	09	05	01	0C	08	04	00

The planetary tables are equi-swept in that the AKR and ITKR radiations fluctuate quite rapidly: the duration of these events does not depend particularly on the frequency.

Table 2: Solar sweep for 32 frequencies

N	y	M	P	list (default)	Sum/Sep	max. frequency no.	average over Z
64	1	8	1	4	0	31	1

1F	1D	1B	19	17	13	0F	07	1E	1C	1A	18	15	11	0B	03
1F	1D	1B	19	16	12	0D	05	1E	1C	1A	18	14	10	09	01
1F	1D	1B	19	17	13	0E	06	1E	1C	1A	18	15	11	0A	02
1F	1D	1B	19	16	12	0C	04	1E	1C	1A	18	14	10	08	00

Table 3: SUM/SEP solar sweep

N	y	M	P	list (default)	Sum/Sep	max. frequency no.	average over Z
64	1	8	1	1	80 (hexa)	15	1

0F	8F	0E	8E	0C	8C	07	87	0F	8F	0D	8D	0A	8A	03	83
0F	8F	0E	8E	0B	8B	06	86	0F	8F	0D	8D	09	89	02	82
0F	8F	0E	8E	0C	8C	05	85	0F	8F	0D	8D	0A	8A	01	81
0F	8F	0E	8E	0B	8B	04	84	0F	8F	0D	8D	08	88	00	80

3.5.3.6.2. RAD2 receiver

Table 0: Solar sweep, RAD2 $0 \times \boxed{16} + 2 \times \boxed{8} + 4 \times \boxed{4} + 6 \times \boxed{2} + 4 \times \boxed{1} = 48$

N	y	M	P	list (default)	Sum/Sep	max. frequency no.	average over Z
8	1	8	6	0	0	15	1

0F	0D	09	0E	0C	07	0F	0B	05	0E	0A	03
0F	0D	08	0E	0C	06	0F	0B	04	0E	0A	01
0F	0D	09	0E	0C	07	0F	0B	05	0E	0A	02
0F	0D	08	0E	0C	06	0F	0B	04	0E	0A	00

Table 1: Planetary Sweep (Equi-sweep list) $16 \times \boxed{3} = 48$

N	y	M	P	list (default)	Sum/Sep	max. frequency no.	average over Z
8	1	8	6	1	0	15	1

0F	0B	07	03	0E	0A	06	02	0D	09	05	01	0C	08	04	00
0F	0B	07	03	0E	0A	06	02	0D	09	05	01	0C	08	04	00
0F	0B	07	03	0E	0A	06	02	0D	09	05	01	0C	08	04	00

Table 2: Solar sweep $0 \times \boxed{16} + 2 \times \boxed{8} + 4 \times \boxed{4} + 6 \times \boxed{2} + 4 \times \boxed{1}$

N	y	M	P	list (default)	Sum/Sep	max. frequency no.	average over Z
12	1	12	4	0	0	15	1

0F	0D	09	0E	0C	08	0F	0B	07	0E	0A	06
0F	0D	05	0E	0C	04	0F	0B	03	0E	0A	01
0F	0D	09	0E	0C	08	0F	0B	07	0E	0A	06
0F	0D	05	0E	0C	04	0F	0B	02	0E	0A	00

Table 3 : Solar sweep

N	y	M	P	list (default)	Sum/Sep	max. frequency no.	average over Z
12	1	6	4	2	0	15	1

0B	0A	09	08	07	05	0B	0A	09	08	06	04
0B	0A	09	08	07	03	0B	0A	09	08	06	01
0B	0A	09	08	07	05	0B	0A	09	08	06	04
0B	0A	09	08	07	03	0B	0A	09	08	06	00

This table does not contain the pointers C, D, E and F. This means that the other 12 frequencies will be further scanned. Due to design oversight, frequency #2 is missing from this list.

Table 4: Solar sweep, SUM/SEP

N	y	M	P	list (default)	Sum/Sep	max. frequency no.	average over Z
8	1	8	6	0	0	15	1

0F	8F	0C	8C	07	87	0E	8E	0A	8A	03	83
0F	8F	0B	8B	06	86	0D	8D	09	89	02	82
0F	8F	0C	8C	05	85	0E	8E	0A	8A	01	81
0F	8F	0B	8B	04	84	0D	8D	08	88	00	80

Table 5: Planetary sweep, (equi-sweep list)

$$12 \times 4 = 48$$

N	y	M	P	list (default)	Sum/Sep	max. frequency no.	average over Z
12	1	12	4	3	0	15	1

0B	08	05	02	0A	07	04	01	09	06	03	00
0B	08	05	02	0A	07	04	01	09	06	03	00
0B	08	05	02	0A	07	04	01	09	06	03	00
0B	08	05	02	0A	07	04	01	09	06	03	00

Note that there is no scanning of C, D, E, F since only 12 frequencies are scanned.

- Note:

These tables can also be found in the loaders of the assembler program (NS 32 bits) contained in the DPU, or online on the "megastar" machine in the /home/wind directory.

3.5.3.7. Measurement acquisition

3.5.3.7.1. RAD1 receiver

As an example, we consider the case of table 0: N = 64, y = 1, M = 8, P = 1.

During a period of rotation of the probe of about 3 seconds, the following characteristics are obtained in normal mode:

Number of samples S acquired	8
Number of samples S' acquired	8
Number of samples Z acquired	8
Number of bits per sample	8

We have the abbreviated notation for the number of samples: $8 S + 8 S' + 8 Z$.

The different durations involved are:

T1	Waiting time due to synthesizer	50 ms
T2	Acquisition time of a sample S or S'	154 ms
T3 2xT2	= Time to acquire a sample Z ²⁶	308 ms

with $T_1 + 2 \times T_2 = T_1 + T_3 = 358$ ms.

Based on the measurement scheduling algorithm shown above, we have the following figure:

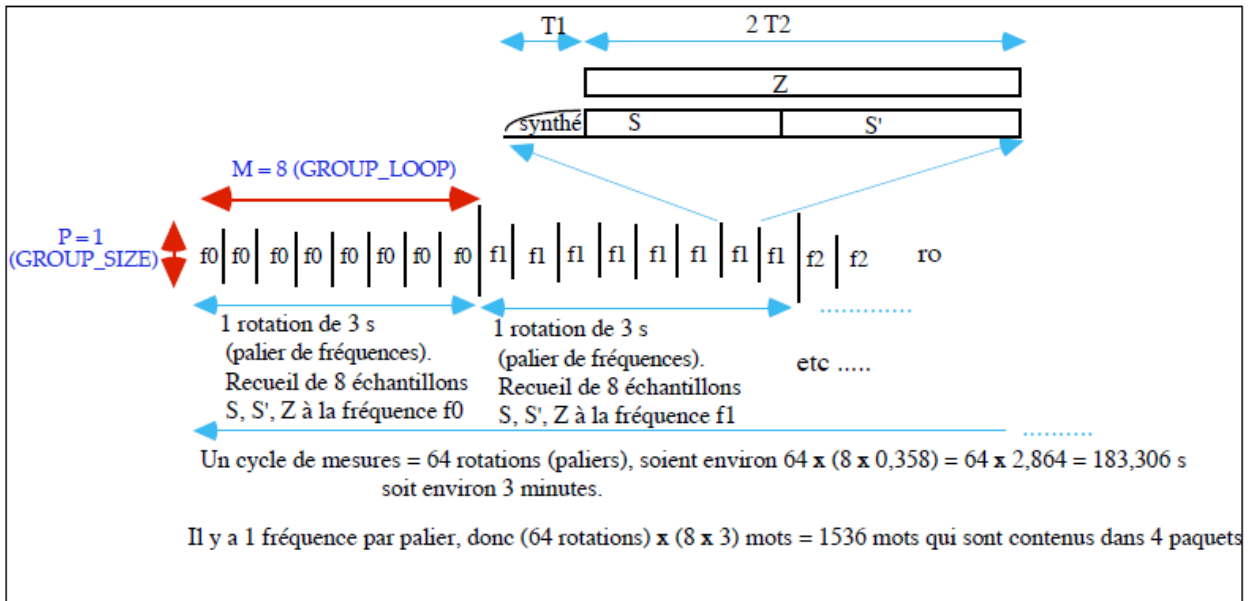


Fig. 1: RAD1, acquisition in normal mode, table 0

Note . The reasons for the choice of the f_i frequencies will be presented in § 3-5-3-8.

At the end of the chapter, an overall view of this ordering is given.

Note that the notion of frequency step only makes sense in the case of the RAD1 receiver, where the data is acquired in a step (rotation) according to the same frequency, which is not the case for the RAD2 receiver.

We have the following calculation:

Number of samples S (or S', or Z) x number of frequencies x ($T_1 + 2 T_2$)

$$= 8 \quad \times \quad 1 \quad \times (0.050 + 2 \times 0.154) \text{ s}$$

$$= 8 \times 1 \times 0.358 = \underline{2.864 \text{ s}} \text{ (about one rotation period of the probe).}$$

1 measurement = (8 S words + 8 S' words + 8 Z words) of 8 bits for 1 frequency (e.g. f_0 above) every 2.864 s

$$= 24 \text{ words of 8 bits for 1 frequency every } 2.864 \text{ s,}$$

$$\text{i.e.: } 24 \times 8 / 2.864 = 67 \text{ bits/s}$$

The possible frequencies are given by the formula: $F_n \text{ (kHz)} = 20 + n \times 4$ with $n = 0$ to 255

²⁶ Integrated all of the time of the acquisition.

Frequency range: 20 to 1040 kHz

Remarks

- for RAD1, as for RAD2, the T_2 integration time is independent of the HBR or LBR telemetry rate, contrary to what was done in the ULYSSE/URAP experiment: when in HBR, the RAD 1/2 receivers have the same acquisition rate.
- the low amplitude signals on RAD1 are noisier on S' than on S (this is related to instrumental problems during design).

Statistical fluctuation rates

The statistical fluctuation rate (rms) for a measurement [STE60] p 42) is valid here:

$$10 \log_{10} \left(1 + \frac{1}{\sqrt{\Delta\nu \cdot T_2}} \right) = 0,1975 \text{ dB} \cong 0,2 \text{ dB}$$

$\Delta\nu$ is the analysis bandwidth before detection, here 3 kHz.

T_2 is the post-detection integration time, here: $T_2 = 154$ ms. Dynamic / number of steps = $90 \text{ dB} / 2^8 = 0.35 \text{ dB}$.

The result is: $0.1975 \text{ dB} < 0.35 \text{ dB}$. In fact, the measurement fluctuations on the received signal should not exceed the value of a signal quantization interval.

3.5.3.7.2. RAD2 receiver

As an example, we consider the case of table 0: $N = 8$, $y = 1$, $M = 8$, $P = 6$.

During a period of rotation of the probe of about 3 seconds, the following characteristics are obtained in the measurement mode²⁷:

Number of samples S acquired	8
Number of samples S' acquired	8
Number of samples Z acquired	8
Number of bits per sample	8

We have the abbreviated notation for the number of samples: 8 S + 8 S' + 8 Z.

The different durations involved are:

T_1	Waiting time due to synthesizer	23 ms
T_2	Acquisition time of a sample S or S'	20 ms

²⁷ Since the data from the Z channel (axial antenna) obviously varies less than that from the S and S' channels, we would have liked to retain only one Z data item out of two, or to average the Z measurements two by two, in order to limit the telemetry rate. In the end, this solution could not be adopted due to lack of time.

$T_3 = 2 \times T_2$	²⁸ Sample acquisition time Z	40 ms
----------------------	---	-------

with $T_1 + 2 \times T_2 = T_1 + T_3 = 63$ ms.

Due to the high frequency range of the RAD2 receiver, these times are obviously much shorter than in the case of the RAD1 receiver, by about 6. This difference is compensated for by: $P = 4$ or 6 . According to the measurement scheduling algorithm (§ 3-5-3-1), we have the following figure:

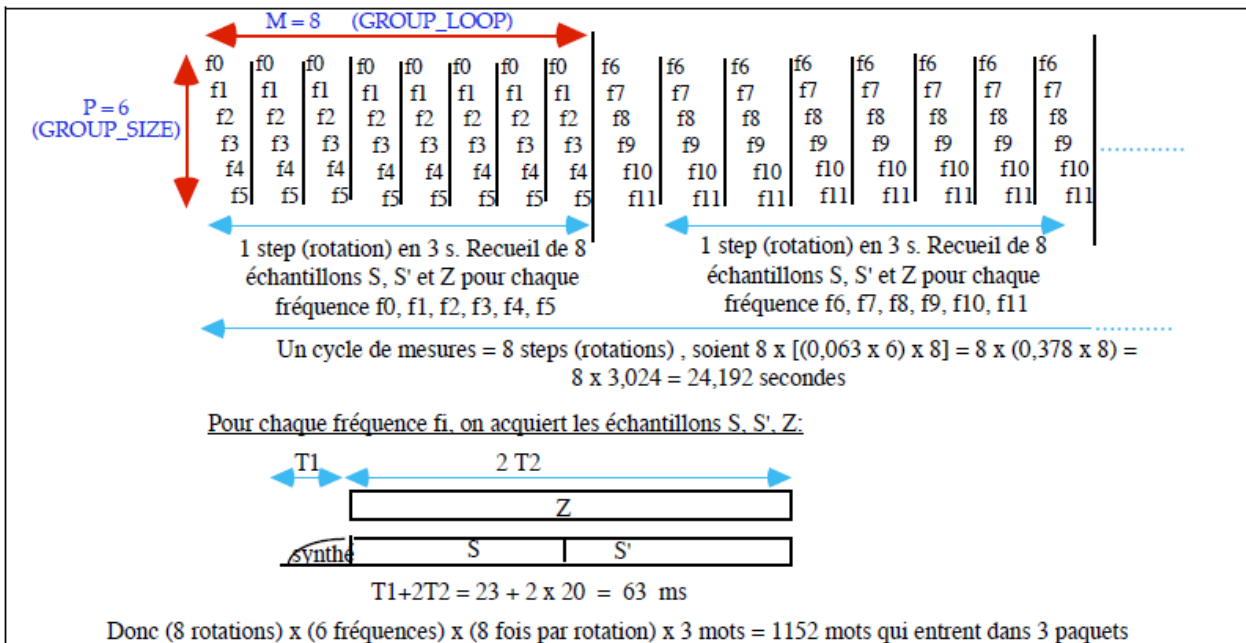


[Fig: RAD2, acquisition in normal mode, table 0](#)

Note The indicated f_i frequencies may reappear from one rotation to the next. The choice of f_i frequencies will be specified in chapter 4. The possible frequencies are given by the following formula: F_n (MHz) = $1.075 + n \times 0.05$ with $n = 0$ to 255

==> Frequency range: 1.075 to 13.825 MHz

At the end of the chapter, a global diagram of this scheduling is presented.

Telemetry rate

We have the following calculation:

$$\begin{aligned}
 & \text{Number of samples } S \text{ (or } S', \text{ or } Z) \times \text{Number of frequencies} \times (T_1 + 2 T_2) \\
 = & 8 \times 4 \times (0.023 + 2 \times 0.020) \\
 = & 8 \times 4 \times 0.063 \\
 = & \underline{3.024 \text{ s}} \text{ (about one rotation period of the probe).}
 \end{aligned}$$

1 measurement = 6 x (8 S words + 8 S' words + 8 Z words), for 6 frequencies, each 3.024 s.
 = 144 words of 8 bits, for 6 frequencies, each 3.024 s, i.e:
 $144 \times 8 / 3.024 = \underline{381 \text{ bits/s}}$

Fluctuation Factor - Dynamics

As with RAD1, the fluctuation factor and the value of a signal quantization interval are compared.

- Fluctuation factor: 0.236 dB
- Dynamic / number of steps = 90 dB / 2⁸ = 0.35 dB

We have: 0.236 dB < 0.35 dB

3.5.3.8. Choice of frequency lists

Different strategies for choosing frequencies are possible: equi-distribution, logarithmic distribution etc... (see next §). In addition, the following constraints must be taken into account for the elaboration of frequency lists:

The frequencies must be chosen from the 256 possible frequencies provided by the synthesizer (RAD1: 20 to 1040 kHz in 4 kHz steps, or RAD2: 1.075 MHz to 13.825 MHz in 50 kHz steps).

The selected frequencies should not be used for interference frequencies: at these frequencies there is a jump in value for S, S' or Z.

3.5.3.8.1. Interference frequencies

The lists of spurious frequencies²⁹ measured on the Engineering Model are as follows:

RAD1

Frequency number	Frequency	Number of points	"Interference" rate in dB above the sensitivity threshold (0.35 dB per point)
7	48 kHz	?	?
9	56 kHz	8 à 15	2,8 à 5,25
11	64 kHz	13	4,55
12	68 kHz	19	6,65
14	76 kHz	6 à 10	2,1 à 3,5
16	84 kHz	60	21
17	88 kHz	22	7,7
19	96 kHz	18	6,3
20	100 kHz	18	6,3
25	120 kHz	10	3,5
27	128 kHz	26	9,1
37	168 kHz	92	32,2
38	172 kHz	89	31,15
45	200 kHz	7	2,45

²⁹ The interfering frequencies are those generated by the converters, which in the case of the RAD1 receiver are multiples of 50 kHz in principle, but in practice are multiples of 100 kHz, due to the 4 kHz frequency step of the frequency synthesizer.

69	296 kHz	27	9,45
70	300 kHz	22	7,7
95	400 kHz	35	12,25
120	500 kHz	50	17,5
143	592 kHz	32	11,2
145	600 kHz	25	8,75
170	700 kHz	49	17,15
195	800 kHz	27	9,45
217	888 kHz	86	30,1
220	900 kHz	60	21
239	976 kHz	30	10,5
245	1000 kHz	40	14
249	1016 kHz	6	2,1
250	1020 kHz	25	8,75
251	1024 kHz	5	1,75
252	1028 kHz	12	4,2

RAD2

Frequency number	Frequency value
104	6,275 MHz
120	7,075 MHz
121	7,125 MHz
122	7,175 MHz
137	7,925 MHz
219	12,025 MHz
220	12,075 MHz

A graphical representation of the different frequency lists is given in the annex.

3.5.3.8.2. Frequency allocation strategies

In addition to the technical constraints mentioned above, the different strategies for choosing the frequencies must be defined. We choose here to generate the frequencies in two ways: equi-distribution or logarithmic frequency distribution.

Let f_{\min} and f_{\max} be the minimum and maximum frequencies of the considered frequency band. For $n + 1$ frequencies, logarithmically distributed between f_{\min} and f_{\max} , we must have

$$\log(f_{i+1}) - \log(f_i) = c^{te}, \quad i = 0 \text{ à } n - 1.$$

Solving this numerical sequence leads to the following distribution:

$$f(i) = f_{\min} \left(\frac{f_{\max}}{f_{\min}} \right)^{i/n} \quad (1)$$

Remark : another possibility would have been to choose $n+1$ frequencies, equally distributed in $1/f$

between f_0 and f_{\max} , so :

$$1/f_{i+1} - 1/f_i = c^{\epsilon}$$

We can verify that we obtain a significant number of frequencies near f_{\min} and a very large spacing between the last frequencies. This has the disadvantage that at low frequencies, solar radio emissions are generally polluted by terrestrial AKR radiation (above about 1/2 A.U., i.e. about 80 to 100 kHz) and the measurements obtained are less reliable. The $1/f$ equi-distribution strategy is therefore questionable in this case.

Details of the frequency values obtained for the different cases: RAD1 or RAD2 receiver, type of distribution, number of frequencies are given in the appendix.

3.5.3.8.3. ULYSSES lists

In order to correlate the in-ecliptic measurements from the WIND/Waves data with the out-of-ecliptic measurements from the ULYSSES/URAP data, a list is constructed for the RAD1 receiver with frequencies that best match the frequencies of the ULYSSES/URAP experiment.

The 12 frequencies of the ULYSSES/URAP high frequency RAR radio receiver are as follows:

(kHz) 52 63 81 100 120 148 196 272 387 540 740 940

Taking into account the interfering frequencies, the following 12 frequencies can be selected for the RAD1 receiver:

(kHz) 52 60 80 104 124 148 196 272 388 540 740 940

In addition, 1040 kHz is added to this list to cover the entire high frequency range of the RAD1 receiver.

To obtain a list of 16 frequencies, we have to choose 3 low frequencies among the possible frequencies which are, in kHz: 20, 24, 28, 32, 36, 40, 44 (the 48 kHz frequency is polluted). We choose the frequencies 20, 28 and 40 (kHz), to avoid that the values are too close.

The final list of the following 16 frequencies is obtained:

Frequency in kHz	20	28	40	52	60	80	104	124	148	196	272	388	540	740	940	1040
Number of frequency	0	2	5	8	10	15	21	26	32	44	63	92	130	180	230	255

Quasi-ULYSSES' list at 16 frequencies

In addition, a new list of 32 frequencies, intended to cover the ULYSSES/URAP receiver frequencies, has been added by download to the RAD1 receiver frequency lists. The list numbers are 8 and 9. This list was used briefly in early 1997. Then on 10/04/1997 at 15:15, a command was uplinked to indicate to the RAD1 receiver the systematic use of this list.

The pointer table is the same: table 2 (32-frequency solar sweep).

Initially intended to be used when the probe is below 150 Earth radius, it was later planned to be used all the time. It has a better match with the frequencies of the ULYSSES/URAP experiment than the 32-

frequency logarithmic list No. 4 and No. 5. This list was composed by M. Reiner [see e-mail from K. Goetz, 10 April 1997]:

Frequency in kHz	20	24	28	32	36	40	44	48	52	60	72	80	92	104	124	136
Number of frequency	0	1	2	3	4	5	6	7	8	10	13	15	18	21	26	29

Frequency in kHz	14	17	19	22	25	27	33	38	42	48	54	62	74	80	94	104
	8	6	6	4	6	2	2	8	8	4	0	4	0	4	0	0
Number of frequency	32	39	44	51	59	63	78	92	10	11	13	15	18	19	23	255

Quasi-ULYSSES" list at 32 frequencies

3.5.3.9. Frequency lists

The following lists are available³⁰:

RAD1

Number of list	Distribution	Number of frequencies
0	logarithmic	16
1	linear	16
2	Quasi-ULYSSES list	16
3	AKR List	16
4-5	logarithmic	2 x 16 = 32
5-7	linear	2 x 16 = 32
8-9	Quasi-ULYSSES list	2 x 16 = 32

RAD2

Number of list	Distribution	Number of frequencies
0	logarithmic	16
1	linear	16
2	logarithmic	12 (completed to 16)
3	linear	12 (completed to 16)
4-5	logarithmic	2 x 16 = 32
5-7	linear	2 x 16 = 32

The frequency values are given below. Their justification is given in the appendix.

³⁰ List n° 0 is the most commonly used list a priori
Chapter 3 – The RAD1 and RAD2 Receivers

RAD1 Lists

frequency coding

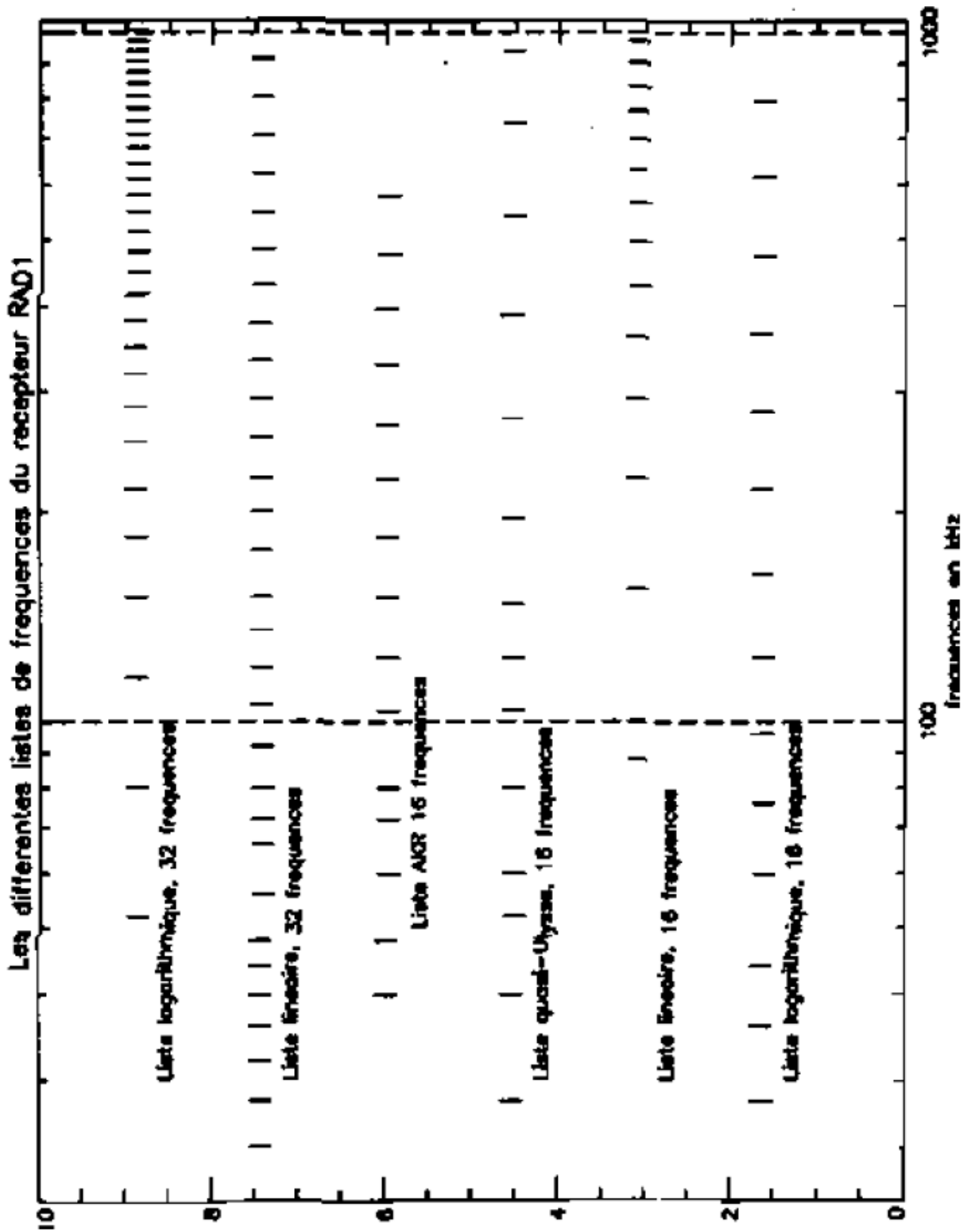
	0	1	2	3	4	5	6	7	8	9	A	B	C	D	E	F
list 0	20	28	36	44	60	76	96	124	164	216	280	364	472	616	796	1040
list 1	20	88	156	224	292	360	428	496	564	632	700	768	836	904	972	1040
list 2 (ULYSSES)	20	28	40	52	60	80	104	124	148	196	272	388	540	740	940	1040
list 3	40	48	60	72	80	104	124	152	184	224	268	328	396	476	580	1040
list 4	20	24	28	32	36	40	44	48	56	66	72	80	92	106	120	136
list 5 (= 4 continued)	152	176	200	224	256	292	332	376	428	484	548	624	708	804	916	1040
list 6	20	52	80	116	152	184	216	252	284	316	348	380	416	448	480	512
list 7 (= 6 continued)	548	580	612	644	680	712	744	776	808	844	876	908	940	972	1008	1040
list 8	20	24	28	32	36	40	44	48	52	60	72	80	92	104	124	136
list 9 (= 8 continued)	148	176	196	224	256	272	332	388	428	484	540	624	740	804	940	1040

RAD2 Lists

frequency coding

	0	1	2	3	4	5	6	7	8	9	A	B	C	D	E	F
list 0	1075	1275	1525	1775	2125	2525	2975	3525	4175	4975	5925	6975	8275	9825	11675	13825
list 1	1075	1925	2275	3625	4775	5325	6175	7025	7875	8725	9575	10425	11275	12125	12975	13825
list 2	1075	1375	1725	2175	2725	3425	4325	5475	6875	8675	10975	13825	11375	11775	12575	13075
list 3	1075	2225	3375	4575	5725	6875	8025	9175	10325	11525	12675	13825	12875	13075	13275	13475
list 4	1075	1175	1275	1375	1475	1625	1775	1925	2075	2275	2475	2675	2875	3125	3425	3675
list 5 (= 4 continued)	4025	4375	4725	5125	5575	6075	6575	7125	7775	8425	9175	9925	10775	11725	12725	13825
list 6	1075	1475	1875	2325	2725	3125	3525	3925	4375	4775	5175	5525	6025	6425	6825	7225
list 7 (= 6 continued)	7675	8075	8475	8875	9325	9725	10125	10525	10925	11375	11775	12175	12575	13025	13425	13825

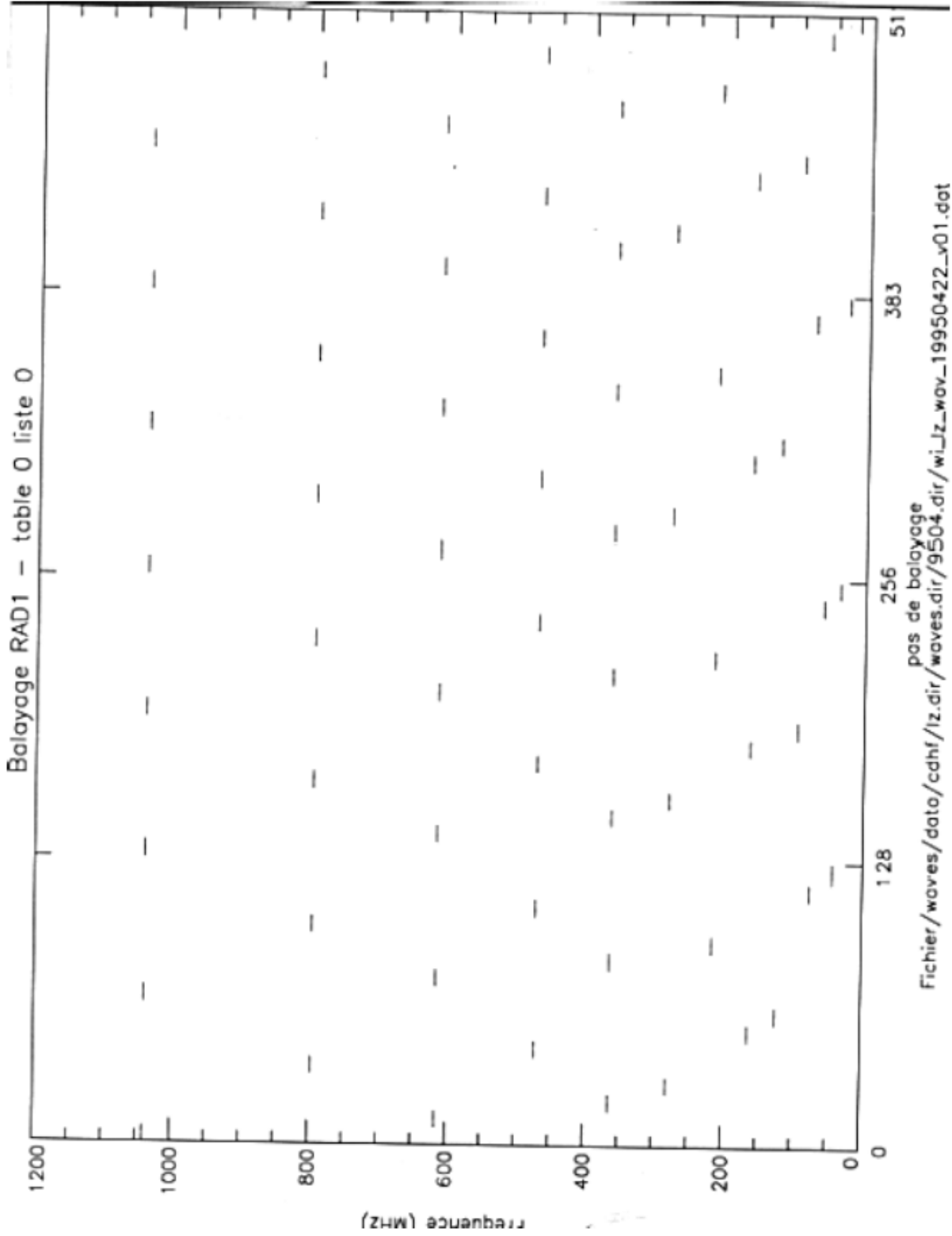
RAD1 receiver frequency lists



RAD1 receiver frequency lists

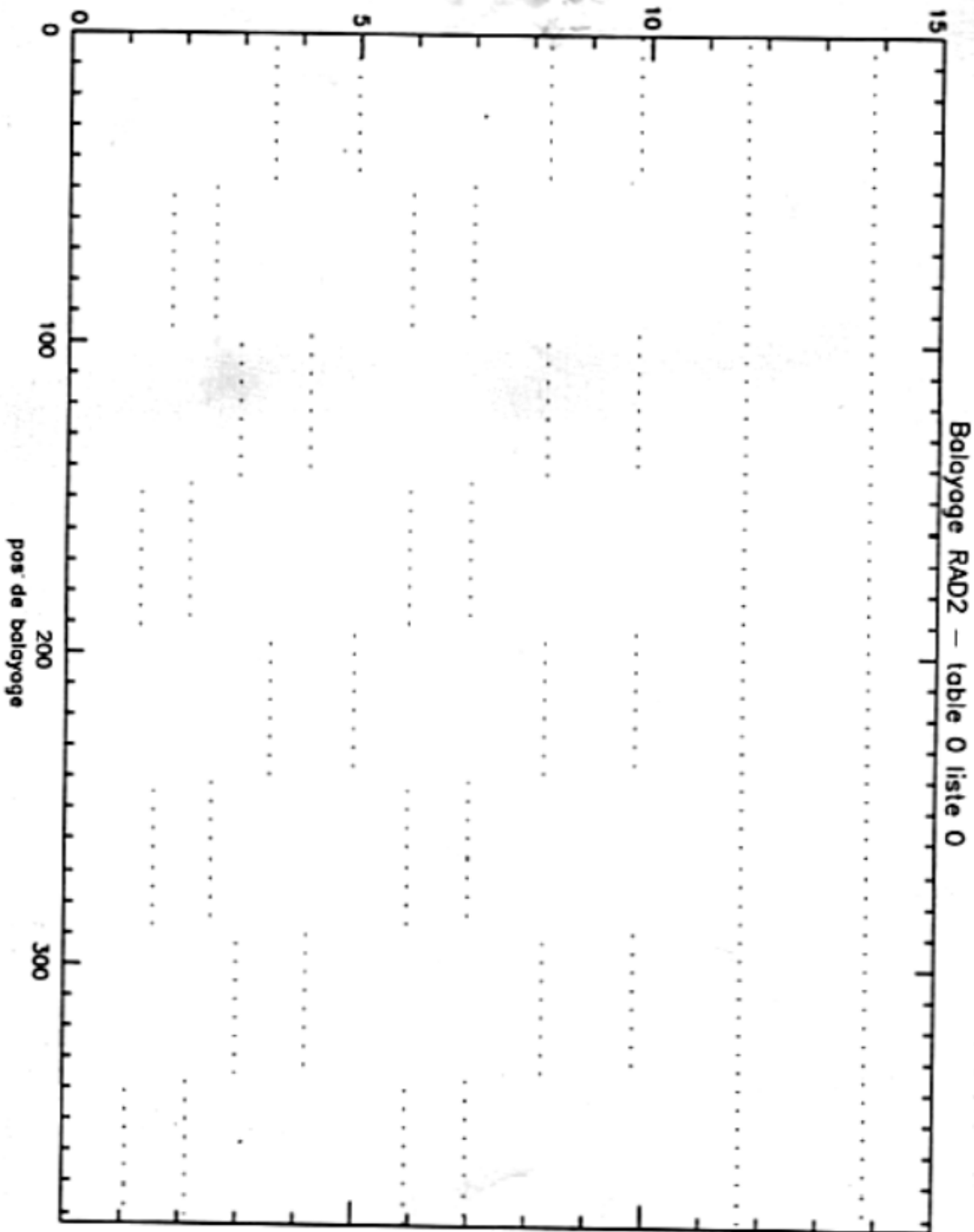
RAD1 Receiver Measurement Scheduling Diagram

N x P x M = 512.



RAD1 Receiver Measurement Scheduling Diagram

N x P x M = 384.



3.5.4. List of "items" for RAD1/2 receivers

The list of items provided by the WIND/Waves³¹ software library for the RAD1 instrument, obtained with the query_database/RAD1 command, is shown below (in alphabetical order). The list of "items" for the RAD2 instrument, which can also be consulted, is more or less identical. It should be noted that these lists evolve regularly.

Constants

DPU CLOCK R4	DPU clock at start of measurement cycle (seconds)
FREQUENCY STEP	Step in the frequency list
INSTR HEADER	Length of instrument header
INTEGRATION TIME S R4	Integration time
MEASURE HEADER	Length of measurement header, 3rd header
NUMBER MEASURES IN SET	Number of measurements in a set
OFFSET TO NEXT SET R4	Time between start of consecutive sets (set of 1)
OFFSET WITHIN SET R4	Time between starts of measurements in a set
PACKET HEADER	Length of packet header
PACKET ID	Number associated with RAD1 packets in primary header
START_OFFSET_SPRIME_R4	Time between EVENT start and the start of the first measurement
START_OFFSET_ZS_R4	Time between EVENT start and the start of the first measurement
SUN ANGLE R4	Sun angle @ event start (degrees)
SUN CLOCK	Dummy 16-bit sun clock which includes both angle and spins
SUN SPINS	Dummy 4-bit spin counter @ event start

Telemetry

ACTUAL MEAS CT	Total number of measurements actually in event
ANTENNA FLAG	Indication of antenna selection (0 = Ex, 1 = Ey)
AUTO MASK	Mask for toggle; after sample, group, cycle, or list
CAL FLAG	Calibration
CHANNEL NUMBERS	Step in the frequency list
DPU CLOCK	24 bits of current DPU clock at start of measurement
DPU MAJOR FRAME	DPU major frame counter at start of measurement
END DPU MAJOR	DPU major frame counter at end of measurement
EVENT_STATE	Event status indicator (fixed tune, linear sweep, list (0 = Error, 1 = Fixed Tune, 2 = Linear Sweep, 3 = List))
EXPECT MEAS CT	Expected number of measurements in event
FIRST FREQ NUM	Channel number for first frequency in event
FREQUENCY STEP	Step in the frequency list
FREQ TABLE	Choice of frequency table in frequency stepping (measurer) mode
GROUP LOOP	Number of times the group of pointer table elements is sampled
GROUP SIZE	Number of pointer-table elements sampled in a logical grouping
LAST FREQ NUM	Channel number for first frequency in event
PACKET COUNT	Count of packets in event
POLAR FLAG	Polarization flag 1=on (0 = No Polar, 1 = Polar)
PROGRAM LIST	Pointer table to be employed in stepping through f'
S	Values from S receiver for one measurement cycle
STEPS	Total number of steps in the measurement cycle
SUM FLAG	Flag showing S and Z are summed into S if =0 (0 = SUM,
SUM LOOP	Normally 1, but 2 if a toggle is set for after a whole

³¹ Keith Goetz, Catie Metree, J. Kappler et al.
Chapter 3 – The RAD1 and RAD2 Receivers

SUN_ANGLE	Accurate value of the 4096 sun counter @ event star
SUN_CLOCK	16-bit sun clock which includes both angle and spin
SUN_SPINS	Arbitrary 4-bit spin counter @ event start
S_PRIME	Values of S' during one measurement cycle
TRANSLATION	Number of the translation table (list of frequencies)
XLATE_TABLE	Translation table in frequency stepping (measure) m
XLAT_MASK	15 for 16-element frequency list, 31 for 32-element
Z	Z values from one complete measurement cycle

File

CHANNEL_COVERAGE	List of channel numbers 0-255
CHANNEL_LIST	Contents of freq/translate file of chan nums for li
FREQUENCY_COVERAGE_HZ_R4	List of frequencies in HZ, in ascending order by ch
FREQUENCY_LIST_HZ_R4	Contents of file of frequency/translate lists in Hz
POINTER_LIST	Contents of file containing the pointer lists for l

Function

CHANNEL_NUMBERS	Channel numbers
FREQUENCIES_HZ_R4	Frequencies in Hz
S_PRIME_SCET_R8	SCET'S for each S_PRIME measurement (UR8) -argument
S_SCET_R8	SCET'S for each measurement (Ulysses R8) -arguments
TOGGLE_LIST	*NONE*
Z_SCET_R8	SCET'S for each measurement (Ulysses R8) -arguments

Physical Quantities

SP_DBVOLTS_R4	RAD S Prime values in dB volts
SP_LOGSFU_R4	RAD S Prime values in log(sfu)
SP_LOGWATTS_R4	RAD S Prime values in log(Watts/m ² Hz)
SP_MICROVOLTS_R4	RAD S Prime values in microvolts/sqrt(Hz) at preamp
SP_SFU_R4	RAD S Prime values in solar flux units(sfu)
SP_WATTS_R4	RAD S Prime values in Watts/m ² Hz
S_DBVOLTS_R4	RAD S values in dB volts
S_LOGSFU_R4	RAD S values in log(sfu)
S_LOGWATTS_R4	RAD S values in log(Watts/m ² Hz)
S_MICROVOLTS_R4	RAD S values in microvolts/sqrt(Hz) at preamp
S_SFU_R4	RAD S values in solar flux units(sfu)
S_WATTS_R4	RAD S values in Watts/m ² Hz
Z_DBVOLTS_R4	RAD Z values in dB volts
Z_LOGSFU_R4	RAD Z values in log(sfu)
Z_LOGWATTS_R4	RAD Z values in log(Watts/m ² Hz)
Z_MICROVOLTS_R4	RAD Z values in microvolts/sqrt(Hz) at preamp
Z_SFU_R4	RAD Z values in solar flux units(sfu)
Z_WATTS_R4	RAD Z values in Watts/m ² Hz

XLATE_TABLE: frequency list. FREQ_TABLE: pointer table.

The list of ICP commands for the RAD1 and RAD2 instruments is as follows:

1. RAD1

- 1.1. Sum
- 1.2. Sep
- 1.3. . Polar
 - 1.3.1. We
 - 1.3.2. Off
- 1.4. Antenna
 - 1.4.1. Ex
 - 1.4.2. Ey
- 1.5. . Sweep
 - 1.5.1. Off
 - 1.5.2. On
 - 1.5.3. Fixed_Tune
 - 1.5.4. dFixed_Tune
 - 1.5.5. Linear_Sweep
 - 1.5.6. Start_f
 - 1.5.7. Step_f
 - 1.5.8. Number
- 1.6. Immediate
 - 1.6.1. Sum
 - 1.6.2. Sep
 - 1.6.3. Polar
 - 1.6.3.1. On
 - 1.6.3.2. Off
 - 1.6.4. Antenna
 - 1.6.4.1. Ex
 - 1.6.4.2. Ey
- 1.7. List
 - 1.7.1. On
 - 1.7.2. Table
 - 1.7.3. Xlat
 - 1.7.4. Sum/SEP
 - 1.7.4.1. After_Group
 - 1.7.4.1.1. On
 - 1.7.4.1.2. Off
 - 1.7.4.2. After_Spin
 - 1.7.4.2.1. On
 - 1.7.4.2.2. Off

2. RAD2

- 2.1. . Sum
- 2.2. . Sep
- 2.3. . Polar
 - 2.3.1. On
 - 2.3.2. Off
- 2.4. List
 - 2.4.1. On
 - 2.4.2. Table
 - 2.4.3. Xlat

2.4.4. Sum/SEP

2.4.4.1. After_Group

2.4.4.1.1. On

2.4.4.1.2. Off

2.4.4.2. After_Spin

2.4.4.2.1. On

2.4.4.2.2. Off

2.5. . Sweep

2.5.1. Off

2.5.2. On

2.5.3. Fixed_Tune

2.5.4. dFixed_Tune

2.5.5. Linear_Sweep

2.5.6. Start_f

2.5.7. Step_f

2.5.8. Number

2.6. Immediate

2.6.1. Sum

2.6.2. Sep

2.6.3. Polar

2.6.3.1. On

2.6.3.2. Off